Quantification of late Cenozoic erosion in Denmark based on sonic data and basin modelling

PETER JAPSEN & TORBEN BIDSTRUP

Japsen, P. & Bidstrup, T. 1999–12–20: Quantification of late Cenozoic erosion in Denmark based on sonic data and basin modelling. *Bulletin of the Geological Society of Denmark*, Vol. 46, pp. 79–99. Copenhagen. https://doi.org/10.37570/bgsd-1999-46-08

The amount of section missing because of late Cenozoic erosion is estimated using basin modelling and sonic data from four stratigraphic levels in 68 Danish wells, and is found to be smaller than estimated in previous studies. The missing section increases from zero in the western and southern part of the Danish North Sea to 1000–1200 m towards north-east, on and along the Skagerrak-Kattegat Platform. In a broad intermediate zone, c. 500 m of mainly Paleocene–Miocene sediments are missing where Paleocene sediments subcrop the Quaternary. On the Skagerrak-Kattegat Platform, an additional c. 500 m Upper Cretaceous–Danian Chalk Group were removed where the lower parts of the Chalk are preserved, whereas the missing sediments must have been progressively younger towards south-west where Miocene sediments subcrop the Quaternary. The deep erosion on and along the Skagerrak-Kattegat Platform documents that Neogene uplift and erosion affected the study area prior to glacial erosion during the Quaternary. These results are consistent with Neogene uplift of south Norway as well as of south Sweden centred around the South Swedish Dome that culminates north-east of the Kattegat. There is good correlation between estimates of erosion based on Chalk velocities and on basin modelling. Comparison of different methods indicates that erosion is overestimated when based on sonic data from Lower Jurassic shale in north-eastern Denmark, and this could be due to lithological differences. It is concluded that maximum burial of the Mesozoic succession occurred prior to Neogene erosion throughout the area, and a previous suggestion of deep erosion in the Sorgenfrei-Tornquist Zone during the Late Cretaceous-Paleogene inversion is rejected.

Key words: North Sea Basin, uplifts, erosion, Neogene, velocity, vitrinite reflectance, basin analysis

Peter Japsen [*pj@geus.dk*] *& Torben Bidstrup* [*tb@geus.dk*], *Geological Survey of Denmark and Greenland (GEUS), Thoravej 8, DK-2400 Copenhagen NV.* *19 April 1999.*

Recognition of the Neogene uplift and erosion of Denmark is difficult because its extent is regional (Japsen 1993), and because the effects are overprinted by the erosion due to the subsequent Quaternary glaciations. Consequently, only few related observations are presented in the literature prior to the 1990's. Studies of the Miocene Vejle Fjord Formation led Larsen and Dinesen (1959) to conclude that considerable parts of Fennoscandia – including not only basement, but also sedimentary formations – were eroded in the Neogene. Spjeldnæs (1975) found that uplift of the Fennoscandian Shield in the late Oligocene-Miocene resulted in a large change in the sedimentary environment and in the drift of the coast-line towards the south-west. Nielsen et al. (1986) found that Neogene uplift of Scandinavia caused a high influx of coarse-grained clastics into the Norwegian-Danish Basin.

In recent years the effect of late Cenozoic erosion in Denmark has been quantified by a number of authors who estimated burial anomalies for rocks of different age relative to reference trends indicating the increase of density, sonic velocity or vitrinite reflectance with depth during normal compaction (Jensen & Schmidt 1992, 1993; Japsen 1993, 1998; Michelsen & Nielsen 1993). Erosion was estimated to be from 1 to 2 km for several wells. Jensen & Schmidt (1993)

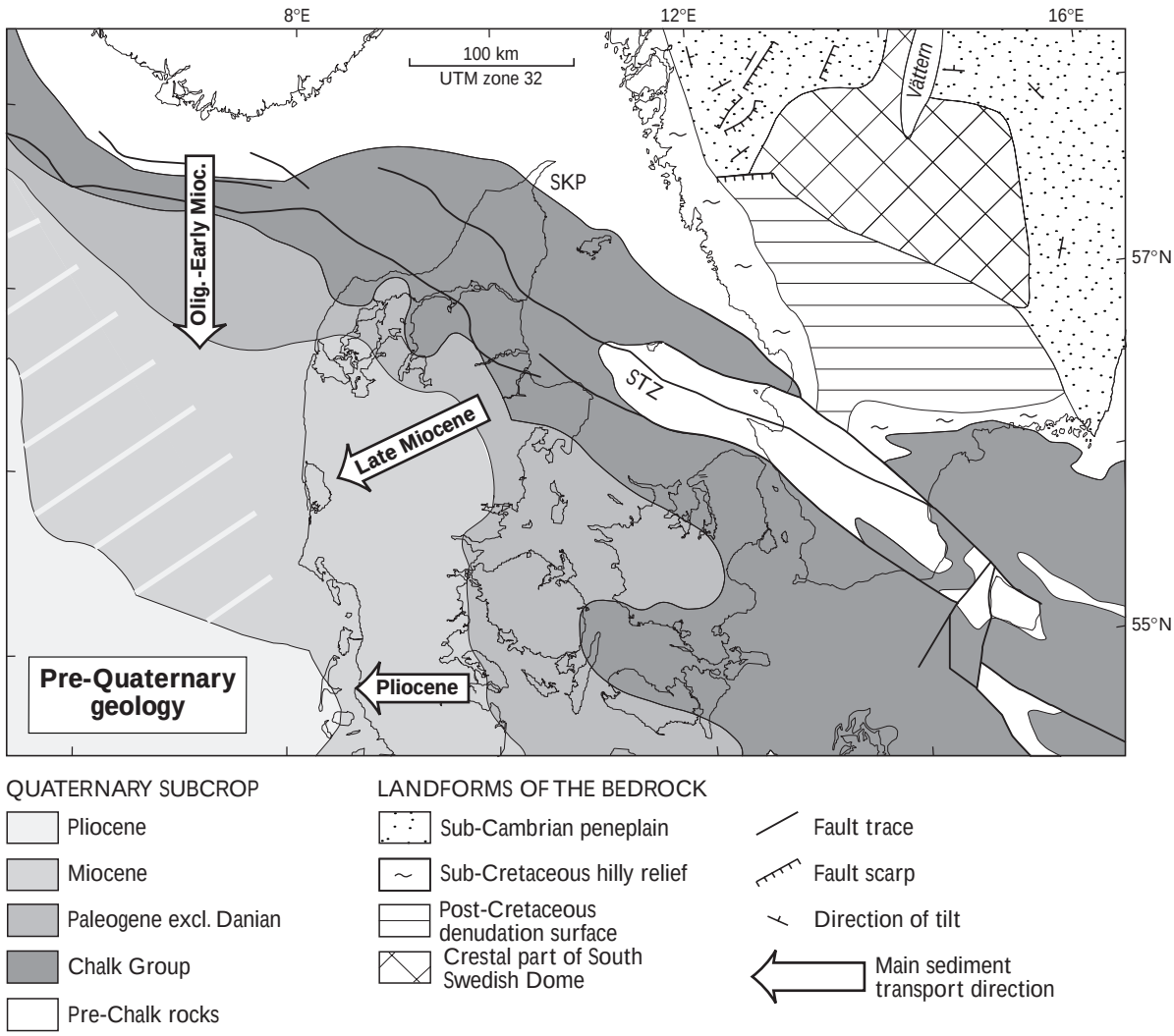

Fig. 1. Pre-Quaternary geology of southern Scandinavia. The change in sediment transport direction from Oligocene to Pliocene time agrees with Neogene uplift of the South Swedish Dome. Note the increasing age of the Quaternary subcrop towards the exposed basement in Norway and Sweden. Modified after Clausen et al. (1999), Fréden (1994), Japsen (1998), Lidmar-Bergström (1996) and Vejbæk & Britze (1994).

presented seismic sections revealing that the effect of pre-Quaternary erosion increases from the central North Sea towards the Norwegian coast, and suggested that this unconformity was related to Neogene uplift of the Norwegian mountains (see Fig. 1). Likewise, Japsen (1993) found the pre-Quaternary surface in Denmark to be an erosional surface created by Neogene uplift and subsequent erosion. Uplift and erosion due to Late Cretaceous-Paleogene inversion was found to be a major component along the Sorgenfrei-Tornquist Zone (Japsen 1993; Michelsen & Nielsen 1993). Japsen (1998) presented a burial-anomaly map based on velocity-depth data for 845 wells for the Upper Cretaceous-Danian Chalk Group in the North Sea Basin. The map revealed an east-west symmetry of the erosional pattern across the North Sea in agreement with the age of the Quaternary subcrop, and this was suggested to indicate that Neogene uplift and erosion affected both margins of the basin. Japsen's (in press) revision of the Chalk baseline leads to a reduction of estimates of erosion by up to 200 m.

This study deals with the timing of maximum burial of the Mesozoic sediments in the Danish area and the magnitude of the subsequent erosion of their cover rocks. We estimate the late Cenozoic erosion based on basin modelling and sonic data from several stratigraphic units in Danish wells (compare e.g. Iliffe & Dawson 1996; Japsen 1998), and get maximum values of 1000–1200 m, which are lower than those found by the studies from the early nineties (Fig. 2). We find that maximum burial of the Mesozoic succession occurred prior to late Cenozoic erosion, and conse-

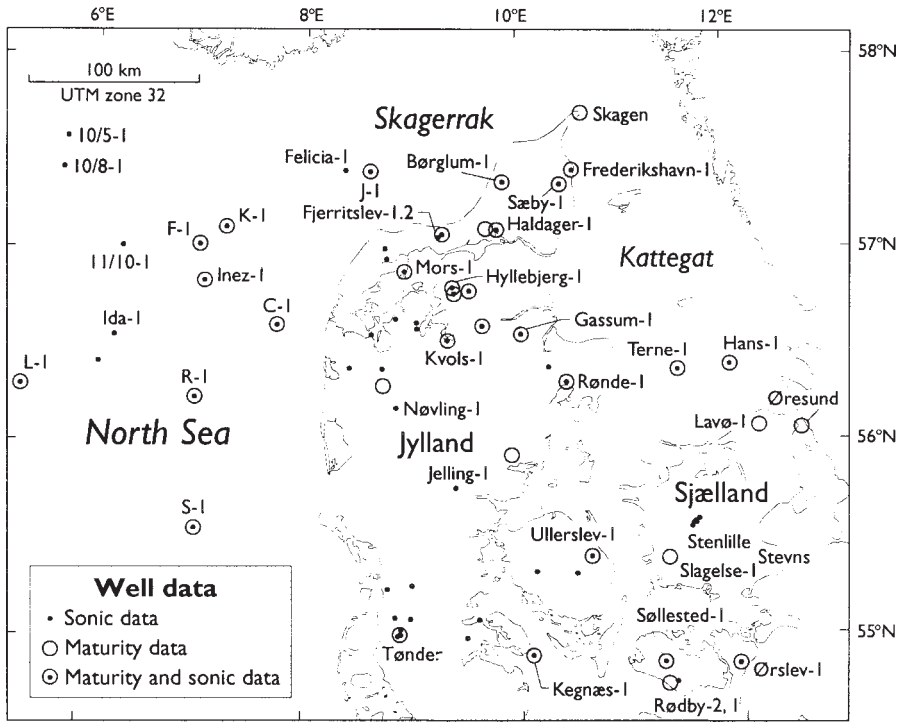

Fig. 2. Place names and location of the 68 Danish and 3 Norwegian wells used in the study. See also well location map in Nielsen & Japsen (1991).

quently, that it is impossible to quantify erosion due to Mesozoic events by the methods applied in the present study.

Erosion estimated from sonic data

Burial anomaly and missing section

A normal velocity-depth trend, $V_N(z)$, may be established for many relatively homogenous sedimentary units saturated with brine (V is sonic velocity [m/s], and z is depth [m]). Such a baseline represents a generalisation which describes the increase of velocity with depth as porosity is reduced during normal compaction (hydrostatic pore pressure, and increasing burial depth with time) (e.g. Bulat & Stoker 1987; Hillis 1995; Japsen 1998, in press). See Appendix A for a discussion of the formulation of baselines for different formations.

The burial anomaly, dZ_B [m], is the difference between the present-day burial depth of a rock, z, and the depth, $z_N(V)$, that corresponds to normal compaction for the measured velocity, V:

$$dZ_B = z - z_N(V) \quad (1)$$

where $z_N(V)$ represents the inverted normal velocity-depth trend for the formation in question (Fig. 3; see list of symbols in Table 1) (Japsen 1998). The burial anomaly is zero for normally compacted sediments. High velocities relative to depth give negative burial anomalies which may be caused by a reduction in overburden thickness ('apparent uplift', Bulat and Stoker 1987; 'net uplift and erosion', Riis & Jensen 1992; 'apparent exhumation', Hillis 1995). A positive burial anomaly may indicate undercompaction due to overpressure.

Whether a burial anomaly is a measure of erosion or is caused by other factors (e.g. lithological changes) is subject to an integrated evaluation of the area in question. Apart from being in agreement with other estimates of erosion, the burial anomalies should also correspond geographically to the extent of a section missing from the stratigraphic record. It must, however, be observed that any post-exhumational burial, B_E [m], will mask the magnitude of the missing overburden section, Δz_{miss} [m], and we get (Fig. 4):

$$\Delta z_{miss} = -dZ_B + B_E \quad (2)$$

where the minus indicates that erosion reduces depth, $dZ_B<0$ (Hillis 1995; Japsen 1998).

Sonic data

Velocity-depth data from 60 Danish wells form part of the data base for this study; these wells are located outside the late Cenozoic depocentre in the central North Sea and outside the Bornholm area in the Baltic Sea (Fig. 2). The data were presented by Nielsen and Japsen (1991), apart from the Ida-1 and Jelling-1 wells. Fifty-two of the wells have interval velocities

Table 1. List of symbols.

B_E	post-exhumational burial
V_0, V_∞	velocity at the surface and at infinite depth
V_N	normal-velocity depth trend for a given formation
V_N^{Ch}, V_N^{BSh}, V_N^{LJur}	normal velocity-depth trends for the Chalk Group, Bunter Shale and lower Jurassic shale (Equations 3–5)
z	present-day burial depth of a rock
z_N	depth corresponding to normal compaction for measured velocity
ΔZ_{miss}	missing section removed by erosion (Equation 2)
${}^{Neo}\Delta Z_{miss}$	missing section removed by late Cenozioc erosion based on sonic data and on basin modelling (Fig. 16)
${}^{Neo}\Delta Z_{miss}^{sonic}$, ${}^{Neo}\Delta Z_{miss}^{bm}$	missing section removed by late Cenozoic erosion based on sonic data or on basin modelling (Fig. 16)
ΔZ_Q	thickness of Quaternary deposits
dZ_B	burial anomaly relative to a normal velocity-depth trend (Equation 1)
${}^{Neo}dZ_B$, ${}^{Neo}dZ_B^{sonic}$	burial anomaly caused by late Cenozioc erosion: based on sonic data and basin modelling, or based on sonic data only (Fig. 16)
dZ_B^{BSh}, dZ_B^{BSs}	Bunter Shale and Bunter Sandstone burial anomaly relative to V_N^{BSh} (Equation 5)
dZ_B^{LJur}, ΔZ_{miss}^{LJur}	burial anomaly and missing section from lower Jurassic shale relative to (Equation 4)
dZ_B^{Ch}, ΔZ_{miss}^{Ch}	Chalk burial anomaly and missing section relative to V_N^{Ch} (Equation 5)
dZ_B^{pre-Ch}	pre-Chalk burial anomaly from lower Jurassic, Bunter Shale and Bunter Sandstone data (Fig. 16)
dZ_{p-B}^{pre-Ch}	pre-Chalk palaeo-burial-anomaly (= $dZ_B^{pre-Ch} - dZ_B^{Ch}$)
dZ_B^{Tr}, ΔZ_{miss}^{Tr}	Triassic burial anomaly and missing section from Bunter Shale and Sandstone data (Fig. 16)

for the Chalk Group, 31 for the F-I Member of the Lower Jurassic Fjerritslev Formation (Michelsen 1989), and 22 for the Bunter Sandstone or the Bunter Shale (Bertelsen 1980); 42 wells have data from the Chalk as well as from the pre-Chalk interval. Three wells have data for all three stratigraphic levels. Data from Danish wells in the central North Sea, and from three Norwegian wells with Chalk velocity data are included in the study to support the contouring. Plots of interval velocities versus midpoint depth for the Chalk Group, the F-I Member, and the Bunter Shale and Sandstone are shown in Figures 5–7.

Chalk burial anomalies are calculated relative to the revised Chalk baseline developed by Japsen (1998, in press) (Equation 3 in Appendix A). Anomalies for the pre-Chalk formations are calculated relative to baselines suggested by Japsen (in press): Burial anomalies for the Lower Jurassic based on data for the F-1 Member relative to the shale trend given by Equation (4), and for the Bunter Sandstone and the Bunter Shale relative to the Bunter Shale trend given by Equation (5).

A single burial anomaly due to late Cenozoic erosion is estimated for each well, and corrected for the Quaternary reburial to obtain an estimate of the missing section (Equation 2; Fig. 4). See the discussion in Appendix B and the results in Table 2.

Erosion estimated from basin modelling

General model considerations

We have modelled the basin development for wells in the study area with a 1D Yükler Model (Yükler 1978). The model is based on a forward modelling program, which means that the programme starts simulation of the geological development from the base of the sedimentary section and performs a calculation forward in time of such parameters as formation thickness, pressure, temperature, vitrinite reflectance, sterane- and hopane-isomerisation ratios and hydrocarbon generation. In order to constrain the results, the calculated values for the present-day situation are compared

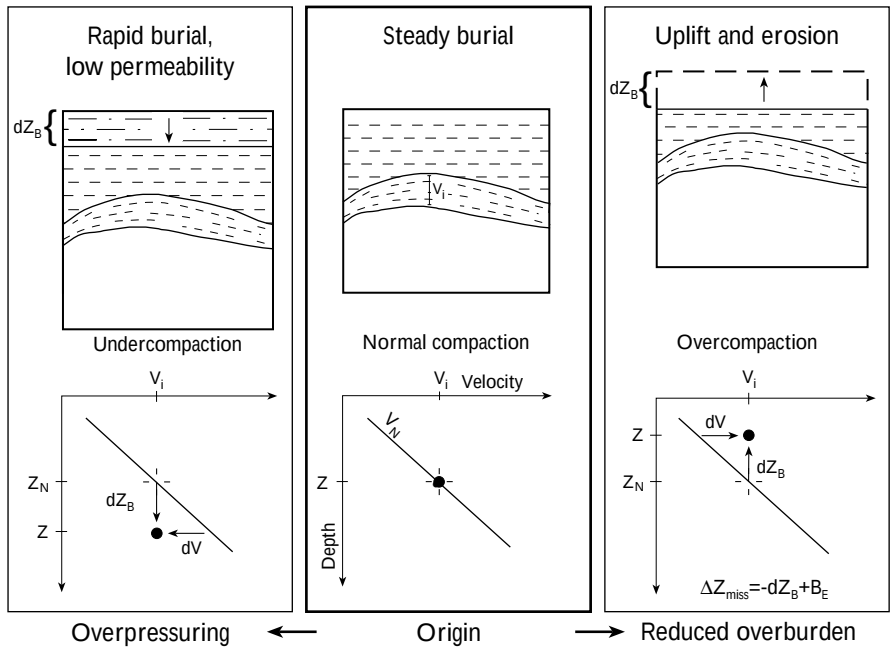

Fig. 3. Velocity anomaly, *dV*, and burial anomaly, dZ_B, relative to a normal velocity-depth trend, V_N. Uplift and erosion reduce the overburden thickness, and cause overcompaction expressed as velocities high relative to depth (negative dZ_B). However, post-exhumational burial, B_E, will mask the magnitude of the missing section, Δz_{miss} (Equation 2; Fig. 4). Undercompaction due to rapid burial and low permeability causes overpressure and velocities low relative to depth (positive dZ_B). The normalised depth, z_N, is the depth corresponding to normal compaction for the measured velocity. Modified after Japsen (1998).

with measured data. Such calibration data can be divided into two groups:

- Data that constrain the thermal history: present-day temperature and thermal maturity data (i.e. vitrinite reflectance values, sterane- and hopane-isomerisation ratios and fission track length distributions).
- Data that constrain the compaction of the sediments: pressure and porosity.

Information on temperature and pressure conditions are normally available in most wells, whereas maturity data are much more scarce. In the study area, vitrinite reflectance data are by far the most common maturity indicator and the study was thus mainly based on temperature and vitrinite reflectance. Due to the varying data quality and sometimes conflicting data values, a manual optimisation procedure was preferred. In the optimisation, high priority was given to obtain a general match to as many different data points as possible and to have a consistent heat flow and erosion model for the area. In the case of conflict between thermal indicator data vitrinite reflectance was given priority.

The 1D modelling programme quantifies and describes all important basin processes as a function of time, and the basin development is thus defined in terms of chronostratigraphic units (model layers or events). The events have the same duration through the entire model area, whereas all other parameters can vary laterally. The total number of events in the geological model, including periods of deposition, non-deposition and erosion must be chosen in such a way that all major geological changes can be described and related to existing stratigraphy. The time and depth resolution should be chosen in such a way that important geological events with short duration and small thickness can be represented.

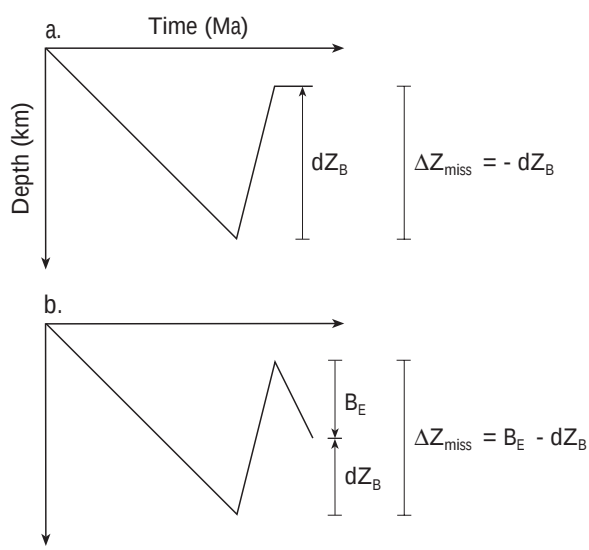

Fig. 4. Schematic burial diagrams illustrating that the magnitude of the missing overburden section (Δz_{miss}) will be less than the magnitude of the measured burial anomaly (dZ_B) in the case of post-exhumational burial (B_E) (Equation 2).
a) Erosion followed by no-deposition.
b) Erosion followed by reburial.

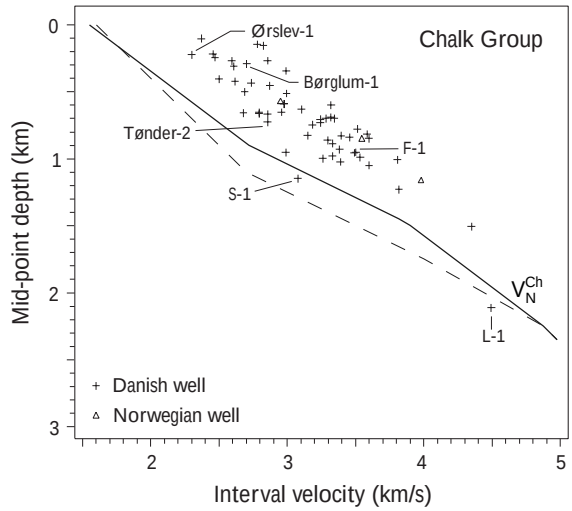

Fig. 5. Interval velocity versus mid-point depth for the Chalk Group, and the revised normal velocity-depth trend for the Chalk, V_N^{Ch} (Equation 3) (Japsen in press). Most data points reveal high velocities relative to the normal trend, and this is suggested generally to be due to overburden reduction. The dashed line indicates the original baseline of Japsen (1998). The revised trend is shifted towards shallower depths by a maximum of 210 m for $2920<V<3920$ m/s.

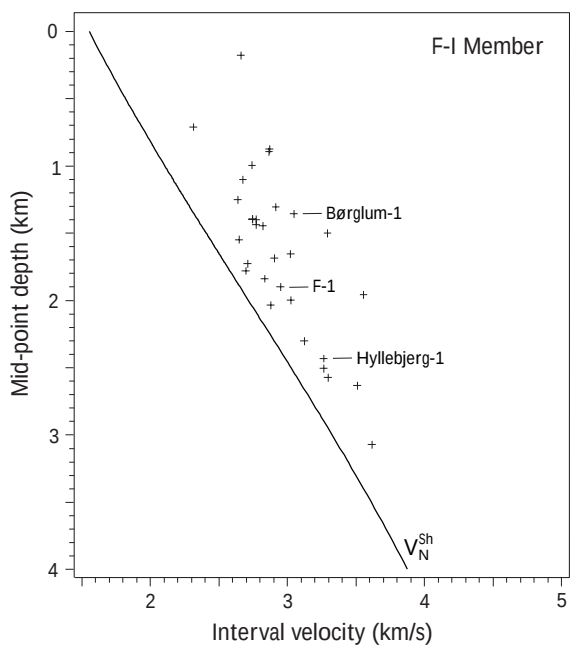

Fig. 6. Interval velocity versus mid-point depth for the Fjerritslev-1 Formation, and the normal velocity-depth trend developed for Lower Jurassic shale, V_N^{LJur} (Equation 4). The trend is within 100 m from the corresponding trend of Scherbaum (1982) that was used by Japsen (1993) for the computation of burial anomalies for the F-1 Member. All data points reveal high velocities relative to the normal trend, and this is suggested to be due to overburden reduction and to an increasing kaolin content towards exposed basement on the Scandinavian Shield.

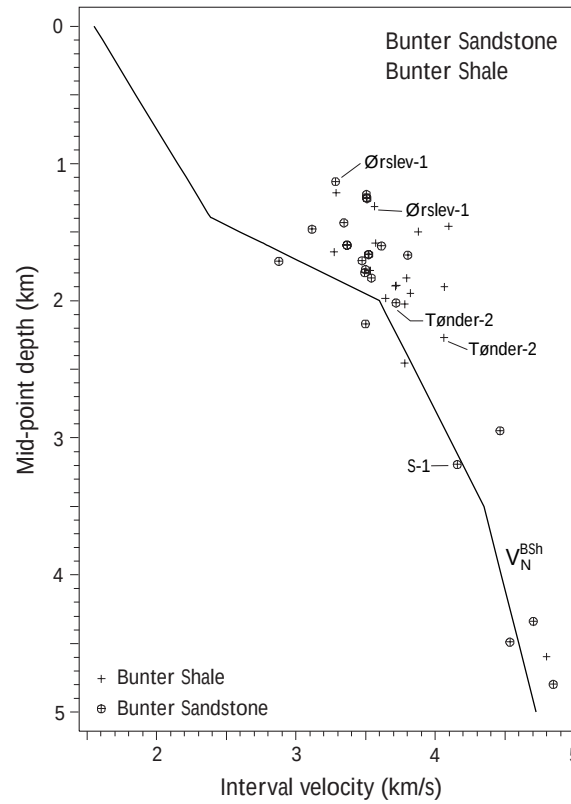

Fig. 7. Interval velocity versus mid-point depth for the Bunter Sandstone and Bunter Shale, and the Bunter Shale trend, V_N^{BSh} (Equation 5). Considerable lithological variations are likely within these formations, but the plot shows a number of data points close to the normal trend and others that plot above the trend generally due to overburden reduction. Note the clear distinction between the Bunter Shale trend and the trend for Lower Jurassic shale in Fig. 6. This difference is suggested to be due to differences in clay mineralogy.

Model description and input data

Definition of events

A total of 45 events was chosen to describe the geological development from the Cambrian until present time within the Danish area using a time step of 250,000 years and a depth step of 25 m (Table 3). The relatively low number of events was chosen as a compromise between the geological details included in the model and the calculation time for the models. The majority of wells in Denmark do not penetrate the entire sedimentary section, for these wells the model has been extended down to basement by the use of seismic data. The lithologies used in the modelling were kept constant for the same event if no geological information dictated otherwise:

Table 2. Burial anomaly and missing section due to Neogene erosion ($^{Neo}dZ_B$ and $^{Neo}\Delta Z_{miss}$) based on estimates from basin modelling and from sonic data ($^{Neo}\Delta Z^{bm}_{miss}$ and $^{Neo}dZ^{sonic}$). The decision tree is depicted in Fig. 16; symbols are explained in Table 1, well locations are indicated on Fig. 2 and in Nielsen & Japsen (1991).

Well	$-\,^{Neo}dZ_B$	$^{Neo}\Delta Z_{miss}$	$^{Neo}\Delta Z^{bm}_{miss}$	$^{Neo}\Delta Z^{sonic}_{miss}$	ΔZ_Q	$-dZ^{sonic}_B$	$-dZ^{Ch}_B$	$-dZ^{LJur}_B$	$-dZ^{BSh}_B$	$-dZ^{BSh}_B$	$-dZ^{pre-Ch}_B$	$-dZ^{pre-Ch}_{p-B}$
Arnum-1	300	400	–	363	44	319	381	–	280	194	194	–188
Års-1	400	500	450	577	122	455	461	442	–	–	442	–20
Borg-1	100	100	–	134	38	96	96	–	–	–	–	–
Børglum-1	900	1000	1000	715	115	600	600	1185	–	–	1185	585
Brøns-1	300	400	–	371	42	329	317	–	299	355	355	38
C-1	400	500	600	424	118	306	306	–	–218	–91	–91	–397
F-1	500	500	600	422	23	399	357	481	–	–	481	124
Farsø-1	500	500	500	512	33	479	530	377	–	–	377	–153
Felicia-1	800	800	–	808	46	762	712	1020	–241	705	[y1]863	151
Fjerritslev-1	800	800	–	793	2	791	791	1352	–	–	1352	561
Fjerritslev-2	500	600	550	815	13	802	802	1443	–	–	1443	641
Frederikshavn-1	700	1000	1000	905	203	702	702	–	–	–	–	–
Gassum-1[z]	700	700	750	604	25	579	579	–	1016	–	1016	437
Glamsbjerg-1	400	500	–	521	126	395	395	–	–	–	–	–
Haldager-1	500	500	550	504	18	486	486	–	–	–	–	–
Hans-1	1100	1200	1200	1807	72	1735	–	1735	–	–	1735	–
Hobro-1	500	600	550	611	68	543	543	–	–	–	–	–
Horsens-1	300	500	450	–	167	–	–	–	–	–	–	–
Hyllebjerg-1	500	500	500	544	19	525	552	470	–	–	470	–82
Ibenholt-1	300	600	–	555	213	342	342	–	–	–	–	–
Ida-1	200	400	–	379	[x]150	229	229	–	–	–	–	–
Inez-1	500	500	600	441	30	411	445	344	–	–	344	–101
J-1	500	600	600	566	36	530	530	1446	–	–	1446	916
Jelling-1	500	500	–	514	[x] 50	464	464	–	288	187	187	–277
K-1	500	600	600	560	76	484	414	624	–	–	624	210
Kegnæs-1	400	400	350	527	28	499	–	–	739	499	499	–
Kværs-1	600	600	–	629	[x] 75	554	–	–	297	554	554	–
Kvols-1	400	500	500	457	57	400	420	361	–	–	361	–60
L-1	0	0	0	0	322	–151	–151	–	–	–	–	–
Lavø-1	400	500	500	–	67	–	–	–	–	–	–	–
Løgumkloster-1	300	400	–	400	64	336	–	–	151	336	336	–
Mejrup-1	300	500	–	476	223	253	264	231	–	–	231	–33
Mors-1	600	700	650	768	136	632	602	690	695	–	692	90
Nøvling-1[y4]	300	400	–	433	[x] 100	333	333	–	–	–	–	–
Oddesund-1	300	500	–	482	174	308	366	194	–	–	194	–171
Øresund	800	800	800	–	[x] 25	–	–	–	–	–	–	–
Ørslev-1	400	400	400	381	19	362	362	–	711	671	671	309
R-1	200	400	500	353	190	163	176	–	137	–	137	–40
Ringe-1	600	700	–	670	91	579	552	–	–	632	632	80
Rødby-1 [z]	500	600	–	578	29	549	473	–	700	1537	700	227
Rødby-2 [y2, z]	500	700	650	–	143	–	–	–	729	1058	1058	–
Rødding-1	400	500	–	523	139	384	400	354	–	–	354	–46
Rønde-1	400	600	550	583	122	461	447	394	582	–	488	41
S-1	0	200	200	0	278	–66	–61	–	–76	–	–76	–15
Sæby-1[y3]	1100	1300	–	1267	216	1051	–	1051	–	–	1051	–
Skagen-1	800	1000	1000	–	219	–	–	–	–	–	–	–
Skive-1	500	600	–	571	78	493	486	506	–	–	506	21
Skive-2	600	700	–	712	74	638	643	627	–	–	627	–17
Slagelse-1	300	500	450	–	102	–	–	–	–	–	–	–
Søllested-1	400	500	450	558	72	486	515	–	429	1034	429	–86
Stenlille-1	600	700	–	655	[x] 50	605	560	693	–	–	693	133
Stenlille-3	600	600	–	636	[x] 50	586	551	656	–	–	656	105
Stenlille-4	600	600	–	608	[x] 50	558	509	656	–	–	656	147
Stenlille-5	600	600	–	623	[x] 50	573	533	653	–	–	653	120
Stenlille-6	600	700	–	673	[x] 50	623	570	729	–	–	729	159
Terne-1	400	500	450	1426	53	1373	–	1373	–	–	1373	–
Thisted-2	500	500	–	546	32	514	514	836	–	–	836	323
Thisted-4	600	700	–	671	31	640	–	640	–	–	640	–

Cont.

Table 2 - Continued

Well	$-^{Neo}dZ_B$	$^{Neo}\Delta Z_{miss}$	$^{Neo}\Delta Z^{bm}_{miss}$	$^{Neo}\Delta Z^{sonic}_{miss}$	ΔZ_Q	$^{-}dZ^{sonic}_B$	$-dZ^{Ch}_B$	$-dZ^{LJur}_B$	$-dZ^{BSh}_B$	$-dZ^{BSh}_B$	$-dZ^{pre-Ch}_B$	$-dZ^{pre-Ch}_B$
Tønder-1	200	200	–	228	45	183	222	–	–74	106	106	–116
Tønder-2	200	300	250	293	48	245	256	–	224	657	224	–33
Tønder-3	300	300	–	319	[x] 45	274	296	–	230	–	230	–67
Tønder-5	300	300	–	348	[x] 45	303	287	–	178	335	335	48
Ullerslev-1	400	500	450	468	47	421	421	–	–	–	–	–
Varnæs-1	400	500	–	525	119	406	–	–	441	406	406	–
Vedsted-1	400	500	450	–	37	–	–	–	–	–	–	–
Vemb-1	200	300	–	267	20	247	238	264	–	–	264	26
Vinding-1	400	500	500	–	59	–	–	–	–	–	–	–
Voldum-1	500	600	–	561	22	539	539	845	–	–	845	306
10/5-1	500	500	–	544	69	475	475	–	–	–	–	–
10/8-1	500	600	–	552	[x] 75	477	477	–	–	–	–	–
11/10-1	400	500	–	485	[x] 75	410	410	–	–	–	–	–

The burial anomaly based on Triassic sonic data, dZ^{Tr}_B, is not shown for simplicity.
[x] Estimated Quaternary thickness
[y1] Triassic burial anomaly from Bunter Shale data
[y2] Well Rødby-2: No estimate of erosion from sonic data. Estimates from pre-Chalk data too high
[y3] Well Sæby-1: Estimate based on Lower Jurassic shale reduced by 500 m
[y4] Well Nøvling-1: Erroneous velocity-depth data for the F-I Member
[z] Salt diapir, possibly local erosion

- Cenozoic events (excluding the Danian): sand and shale with occasional coals; more shaly towards the base of the succession.
- Lower Paleocene and the Upper Cretaceous events: chalk.
- Lower Cretaceous events: a mix of silt, marl and shale.
- Upper Jurassic events (thin or absent in a large part of the area): shale and siltstone.
- Middle Jurassic events: mixed sandstone, siltstone and shale.
- Lower Jurassic events: shale, silt and sandy shale.
- Triassic events: Sand stone, sandy shale to shale with carbonate and carbonate; locally salt.
- Upper Permian events: clean salt if the layer is thick, otherwise a mixture of shale, anhydrites and salt
- Lower Permian to Cambrian events: shale and sandstone.

Only sparse calibration data are available below top Triassic. Only few wells penetrate the Permian therefore lithologies below this level is uncertain.

Paleo-surface-temperatures. The palaeo-surface-temperature is the average temperature of the sediment-water interface during a particular period. Estimates of palaeo-temperature were modified from Buchart (1978), and used in the simulations of all wells (Fig. 8).

Heat flow model. The heat flow at the base of the sedimentary succession is used as input to the model (typically around a depth of 10 km or less). The heat flow at this level is affected by transient effects from sedimentation and erosion, in contrast to the background heat flow from the upper mantle (Vik & Hermanrud 1993). A constant heat flow of 1 HFU (Heat Flow Unit) is used in the simulations from the Cambrian (event 1) until the beginning of the Oligocene (event 34) for all wells in the study. The heat flow model for the Oligocene–Recent time interval is modified to match present-day temperature and vitrinite reflectance data, but constrained to result in smooth heat flow variations in time and space.

Erosion model. Vitrinite reflectance is much more sensitive to temperature than to time, and therefore depends mainly on maximum temperature and not on when this temperature was reached; i.e. when the sediments were at maximum burial. The timing of erosion subsequent to maximum burial must thus be based on the existing stratigraphy and on general geological considerations. A model of erosion starting in the Late Miocene and continuing until the late Quaternary has been used. See the discussion in the section Timing of Maximum Burial.

Model calibration and results

Basin modelling was performed for wells where the heat flow and erosion model could be calibrated against temperature and vitrinite data available from the in-house data base at GEUS. The quality and the number of temperature and vitrinite measurements in the wells vary greatly, and 35 wells (including the Øresund profile; Larsen 1966) were found to have sufficient data to calibrate the model (Fig. 2; Table 2). Examples of the match between calculated and meas-

Table 3. Subdivision of the sedimentary record into model layers/events used for the basin modelling. 'BM time' is the time scale in million years used for the definition of the events (Haq et al. 1987; Harland et al. 1990).

TIME-SCALE		*EVENT SPLITTING*		
		BM time	EVENT NAME	E.No.
PLEISTOCENE		0,5	QUATERNARY-3	45
		1,0	QUATERNARY-2	44
		1,5	QUATERNARY-1	43
PLIOCENE	PIACENZIAN	2,0	PLIOCENE-3	42
		3,0	PLIOCENE-2	41
	ZANCLEAN	5,0	PLIOCENE-1	40
MIOCENE	MESSINIAN	7,0	MIOCENE-4	39
	TORTONIAN	10,0	MIOCENE-3	38
	SERRAVALLIAN			
	LANGHIAN	16,0	MIOCENE-2	37
	BURDIGALIAN		MIOCENE-1	36
	AQUITANNIAN	26,0		
OLIGOCENE	CHATTIAN	30,0	OLOGOCENE-2	35
	RUPELIAN	36,0	OLIGOCENE-1	34
EOCENE	PRIABONIAN		EOCENE-3	33
	BARTONIAN	42,0		
	LUTETIAN	49,0	EOCENE-2	32
	YPRESIAN	54,0	EOCENE-1	31
PALEOCENE	THANETIAN	60,0	PALEOCENE-2	30
	DANIAN	66,0	PALEOCENE-1	29
L. CRETACEOUS	MAASTRICHTIAN	72,0	L CRETACEOUS-3	28
	CAMPANIAN		L CRETACEOUS-2	27
	SANTONIAN	86,0		
	CONIACIAN		L CRETACEOUS-1	26
	TURONIAN			
	CENOMANIAN	96,0		
E. CRETACEOUS	ALBIAN		E CRETACEOUS-2	25
	APTIAN			
	BARREMIAN			
	HAUTERIVIAN	117,0		
	VALANGINIAN		E CRETACEOUS-1	24
	BERRIASIAN	129,0		
L. JURASSIC	TITHONIAN	134,0	L JURASSIC-4	23
		140,0	L JURASSIC-3	22
	KIMMERIDGIAN	142,0	L JURASSIC-2	21
	OXFORDIAN	152,0	L JURASSIC-1	20
M. JURASSIC	CALLOVIAN		M JURASSIC-3	19
	BATHONIAN	161,0		
		166,0	M JURASSIC-2	18
	BAJOCIAN		M JURASSIC-1	17
	AALENIAN	178,0		
E. JURASSIC	TOARCIAN	186,0	E	16
	PLIENSBACHIAN	194,0	E JURASSIC-3	15
	SINEMURIAN	201,0	E JURASSIC-2	14
	HETTANGIAN	210,0	E JURASSC-1	13
L. TRIASSIC	RHAETIAN		L TRIASSIC	12
	NORIAN	223,0		
	CARNIAN		M TRIASSIC	11
M. TRIASSIC	LADINIAN			
	ANISIAN	240,0		
E. TRIASSIC	SCYTHIAN	250,0	E TRIASSIC	10
L. PERMIAN			L PERMIAN	9
	ZECHSTEIN	256,0		
		265,0	E PERMIAN-4	8
		273,0	E PERMIAN-3	7
		281,0	E PERMIAN-2	6
E. PERMIAN	ROTLIEGENDES	290,0	E PERMIAN-1	5
L. CARBONIFEROUS	PENNSYLVANIAN		CARBONIF/DEVON	4
E. CARBONIFEROUS	MISSISSIPPIAN			
DEVONIAN		408,0		
SILURIAN		439,0	SILURIAN	3
ORDOVICIAN		510,0	ORDOVICIAN	2
CAMBRIAN		570,0	CAMBRIAN	1

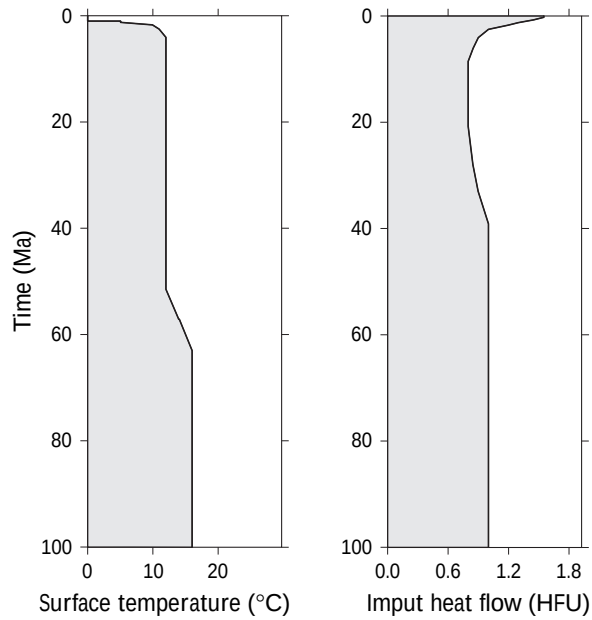

Fig. 8. Plots of palaeo–surface-temperatures and heat flow history used in the modelling of Hyllebjerg-1 well. A heat flow of 1 HFU has been used until the Oligocene, after which heat flow was allowed to change smoothly to match calibration data. The palaeo-surface-temperatures are the same for all wells in the study (modified after Buchart 1978).

ured values of temperature and vitrinite reflectance for 6 wells are shown in Fig. 9. Calibration against pressure data is not important because no overpressure has been observed in the study area.

In general, temperature measurements have been made in all wells as part of the original log-runs. In a few wells special temperature logs have been run a long time after the drilling has stopped. These data may be used to constrain the thermal conductivity of the lithologies. Unfortunately the thermal properties is an integrated part of lithologies in the Yükler model, and cannot be changed at user level. New lithologies constructed and calibrated in individual wells cannot necessarily be used in other wells. Because of the regional character of this study, we have preferred to use standard lithologies and to allow only moderate variations. Therefore, only the general temperature trend has been matched to give an estimate of the present-day heat flow.

The optimisation of the heat flow model resulted in a smooth heat flow variation with time, an example of the heat flow history for the Hyllebjerg-1 can be seen on Fig. 8, and the corresponding calibration plot is shown in Fig. 9. The resulting heat flow distribution are shown for three different times (Fig. 10). In order to match the steep vitrinite reflectance gradients observed in central and northern Jylland low heat flow is used in this area during maximum burial (Late Miocene, c. 10 Ma before present).

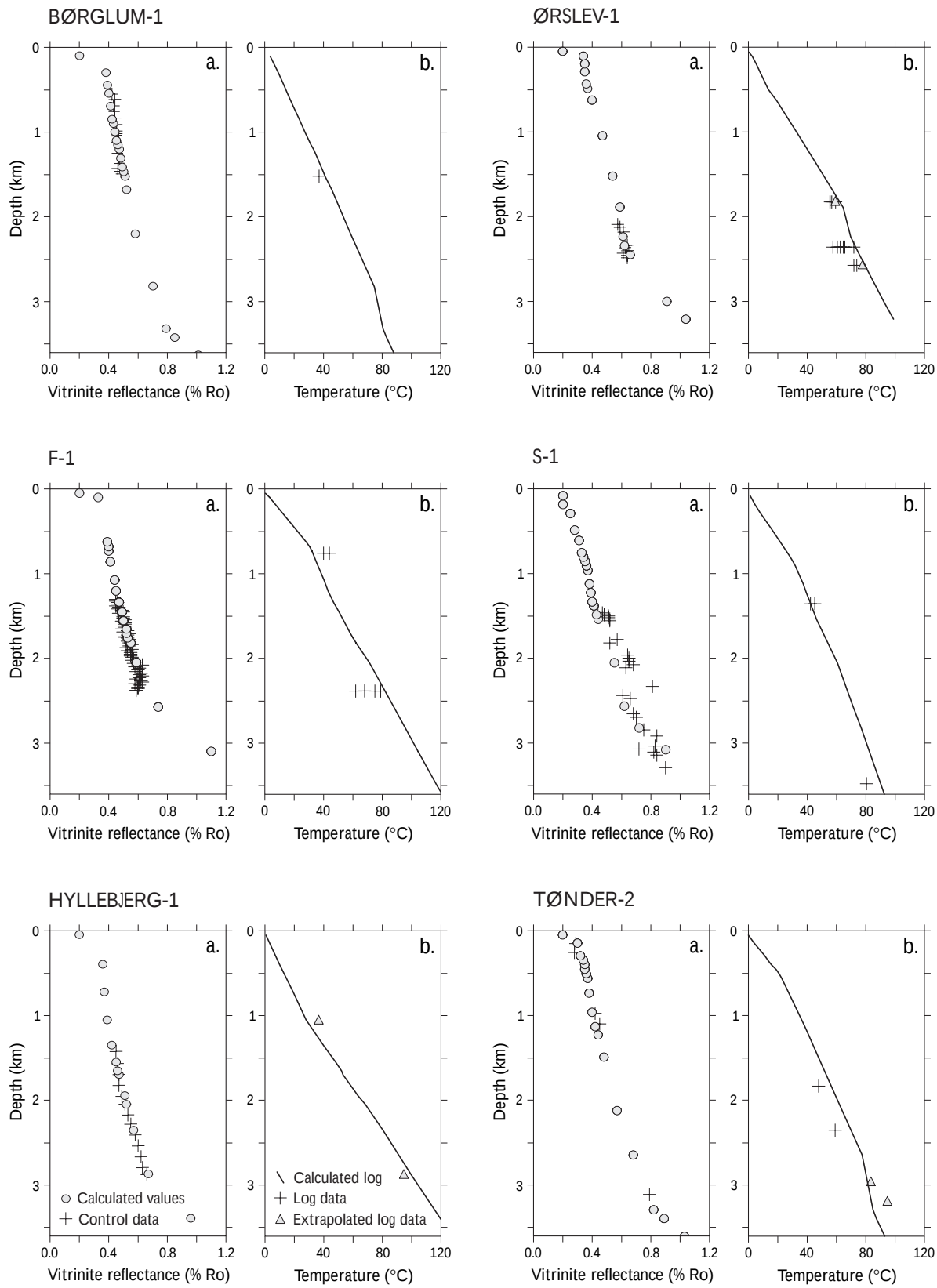

Fig. 9. Plots of calculated and measured values of a) vitrinite reflectance and b) temperature for the wells Børglum-1, F-1, Hyllebjerg-1, Ørslev-1, S-1, Tønder-2.

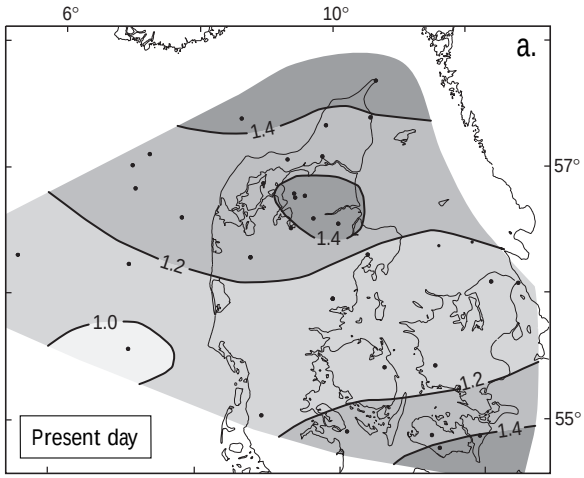

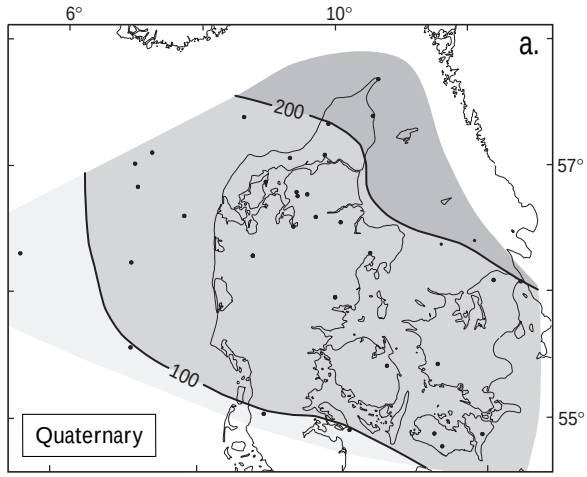

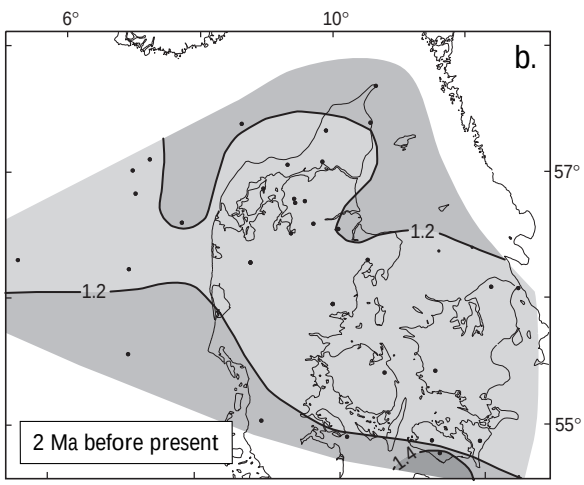

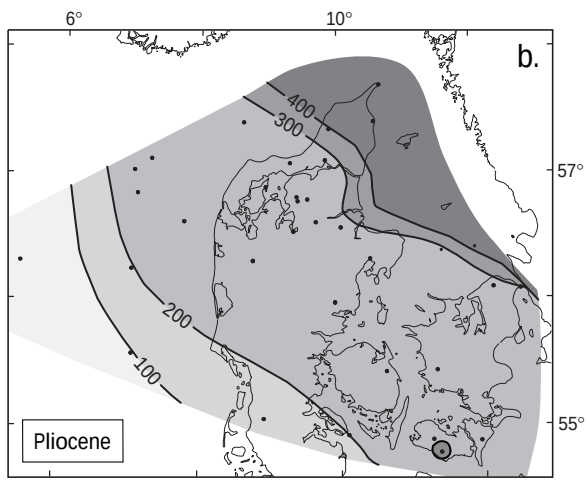

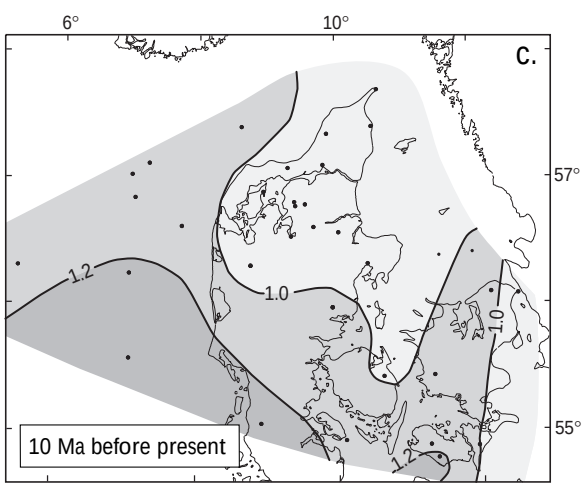

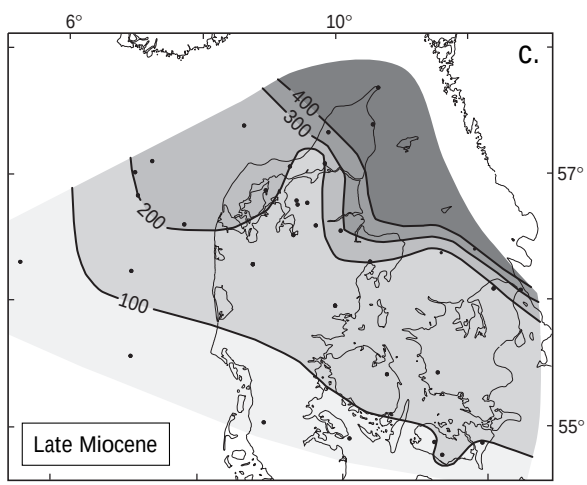

Heat flow

Contour interval 0.2 heat flow units

• Well data

100 km

UTM zone 32

Erosion

Contour interval 100 m

• Well data

100 km

UTM zone 32

Fig. 10. Maps of heat flow at three times during the late Cenozoic predicted by the basin modelling. The heat flow is assumed to be constant until the Oligocene (1 HFU), but through the Oligocene–Recent, heat flow is allowed to vary smoothly to match calibration data.

a) Present day,
b) 2 Ma before present,
c) 10 Ma before present.

Fig. 11 Maps of erosion for three intervals during the late Cenozoic used in the basin modelling. The existing stratigraphy constrains the temporal development of the erosion.

a) Quaternary,
b) Pliocene,
c) Late Miocene.

The small bend of the contours in north-eastern Denmark on all maps is mainly due to the data for the Gassum-1 well, and may reflect a local structure.

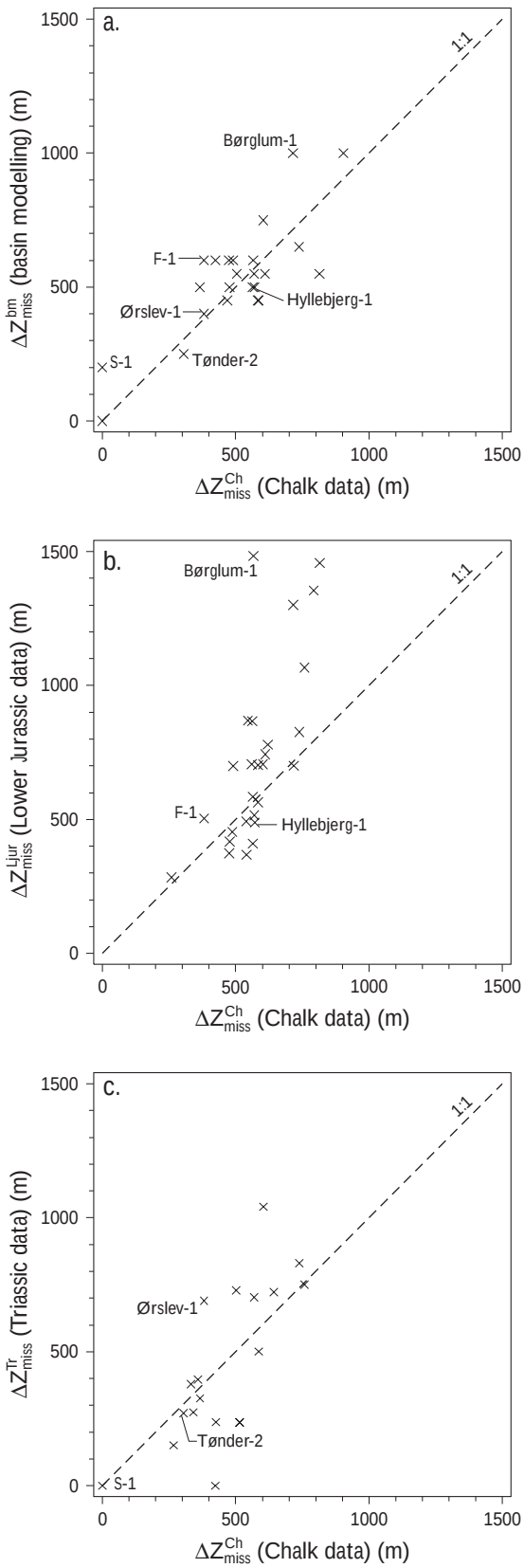

Fig. 12. Correlation between estimates of missing section. Note the good correlation between estimates based on Chalk velocities and basin modelling. Estimates based on data for Lower Jurassic shale are overestimated relative to estimates from Chalk data in north-eastern Denmark.

a) Estimates based on Chalk sonic data, ΔZ^{Ch}_{miss}, versus estimates from basin modelling, ΔZ^{bm}_{miss}.

b) Estimates based on Chalk sonic data, Δz^{Ch}_{miss}, versus estimates based on sonic data for Lower Jurassic F-1 Member, ΔZ^{Ljur}_{miss}.

c) Estimates based on Chalk sonic data, ΔZ^{Ch}_{miss}, versus estimates based on sonic data for Lower Triassic Bunter Sandstone and Bunter Shale, ΔZ^{Tr}_{miss}.

The lines illustrating the 1:1 relationship between the estimates are shown. Well names are annotated for wells with results of basin modelling shown in Fig. 9.

For all wells studied, apart from the L-1 and S-1 wells, calibration of the model required the deposition of overburden sediments and their subsequent removal (Fig. 11; Table 3). For the S-1 well seismic data indicate erosion just west of the well, therefore 200 m erosion has been used in the basin modelling. This erosion is not in conflict with the calibration data. The thickness of the missing section can only be estimated within a range of possible solutions, and this range is constrained by the data quality (e.g. vitrinite data), by the lateral consistency of the model of erosion and heat flow, and by the general geological understanding of the area. The uncertainty on the estimate of erosion is thus typically in the order of 100-200 m.

Estimates of missing section due to late Cenozoic erosion

Comparison of estimates of missing section

Estimates of the missing section based on Chalk data and on basin modelling are quite similar (Table 3); the correlation coefficient is 0.81 for the 24 data points and the mean difference between the estimates is 30±130 m (Fig. 12a). The estimates of the missing section based on Chalk data and on Triassic data are also rather similar, but the scatter is greater; the correlation coefficient is 0.72 for the 19 data points and the mean difference between the estimates is 10±210 m (Fig. 12c). The estimates of the missing section based on Chalk data are generally smaller that those based on Lower Jurassic data; the correlation coefficient is 0.71 for the 27 data points and the mean difference between the estimates is 150±270 m (Fig. 12b).

Only in north-eastern Denmark does the magnitude of the pre-Chalk burial anomaly generally exceed the estimates from Chalk data and basin modelling; e.g. differences of 500-1000 m between anomalies for the Chalk and the F-1 Member. A possible interpretation

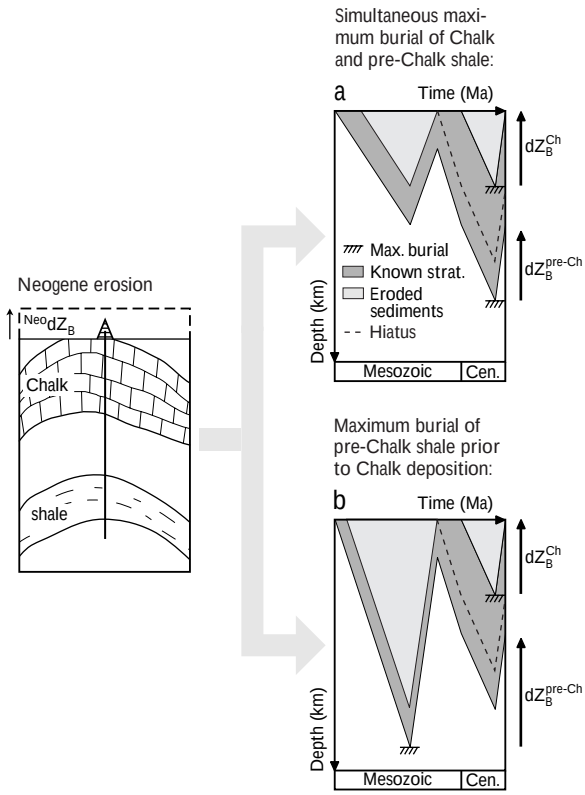

Fig. 13. Schematic burial diagrams for the Mesozoic succession illustrating the relationship between burial anomalies for the Chalk and a pre-Chalk shale, dZ_B^{Ch} and dZ_B^{pre-Ch}, in the same well under the assumption of no major lateral variations in lithology. Either the two units have been at maximum burial depth simultaneously or the lower unit has been at maximum burial prior to the upper unit due to an intervening erosional event.

a) $dZ_B^{Ch} = dZ_B^{pre-Ch}$ indicates that the maximum burial of these layers was simultaneous.

b) $-dZ_B^{Ch} = <-dZ_B^{pre-Ch}$ indicates that the pre-Chalk sediments experienced maximum burial prior to deposition of the Chalk. Modified after Japsen (in press).

of this difference could be that the Lower Jurassic in the area experienced maximum burial prior to the deposition of the Chalk (Fig. 13). It is, however, not possible to identify a major hiatus in the stratigraphic record corresponding to a deep erosional event that could explain the difference between the Chalk and the pre-Chalk burial anomalies (e.g. the Fjerritslev-1 well where an almost complete Jurassic–Lower Cretaceous succession is present; compare Nielsen & Japsen 1991). Furthermore, there is a general agreement between the erosional estimates based on sonic data from the Chalk and those from basin modelling in northern Jylland as in the rest of Denmark. Lateral lithological variations within the F-I Member are likely causes for the observed high estimates of erosion based on sonic data from that formation. Maximum burial of the Mesozoic succession thus occurred during the Cenozoic throughout the study area.

Japsen (in press) argued that the water adsorbed on the smectite/illite particles could lead to weak mechanical grain contacts, and thus to the low sonic velocity generally observed for Lower Jurassic shale at depth (compare Fig. 6). However, the kaolin-dominated, Bunter Shale has a much higher velocity at depth (Fig. 7). An increase in the kaolin content of the Lower Jurassic shale towards exposed basement on the Scandinavian Shield could thus be a possible explanation for the relatively high velocity of the F-I Member in north-eastern Denmark. This also agrees with the more shallow marine environment found towards the north and east in the earliest Jurassic (Pedersen 1985; Lindgreen 1991).

The high velocities of the F-I Member has previously been suggested to reflect maximum burial prior to Late Cretaceous-Paleogene inversion within the Sorgenfrei-Tornquist Zone and the subsequent removal of 1 km Chalk (Japsen 1993; Michelsen & Nielsen 1993). Removal of a thick Chalk section during the inversion of the Zone is, however, also unlikely because seismic events within the Chalk section onlap an anticlinal structure along the Sorgenfrei-Tornquist Zone in the western parts of the Kattegat (Liboriussen et al. 1987). Syn-depositional growth of the inversion structure, with peak movements during mid-Cretaceous times, implies that only a thin Chalk section was deposited in the inversion zone.

Timing of maximum burial and subsequent erosion

Along the margins of the North Sea Basin, the Chalk was at maximum burial prior to Neogene erosion (Japsen 1998). This conclusion applies to the majority of wells in the present study where Chalk overlain by Paleogene sediments is encountered, and where the sonic data for the Chalk indicate a previous greater depth of burial. Here, maximum burial of the Chalk must have occurred during the Cenozoic after the deposition of Paleocene–Miocene sediments.

In south and central Jylland, the timing of erosion can be further detailed because it must post-date the deposition of offshore to shoreface sediments of the Upper Miocene Gram Formation (Rasmussen 1961; Erik S. Rasmussen, personal communication 1999).

The timing of maximum burial is less constrained in and north of the Sorgenfrei-Tornquist Zone where the Chalk is deeply eroded or absent (Fig. 1). This study documents a jump in the magnitude of erosion along the northern side of the Sorgenfrei-Tornquist Zone, and this might indicate an earlier onset of erosion on the Skagerrak-Kattegat Platform, possibly in the Late Miocene (see below; Fig. 14). A much earlier onset of erosion would not allow for the deposi-

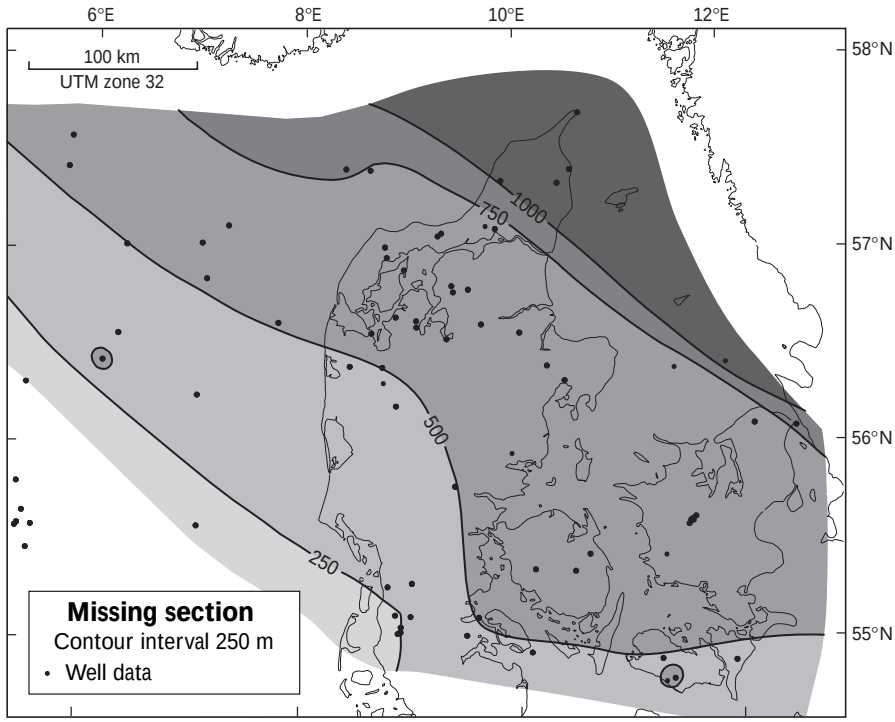

Fig. 14. Map of the section missing due to late Cenozoic erosion based on estimates from basin modelling and sonic data (Table 2). A succession of about 500 m post-Chalk sediments are missing in large parts of the study area. Towards north-east, c. 1000 m are missing where the Chalk is missing or deeply eroded on the Skagerrak-Kattegat Platform and along the northern side of the Sorgenfrei-Tornquist Zone. Only in the south-western part of the Danish North Sea sector no erosion occurred.

tion of the c. 500 m Cenozoic sediments missing just south of the Sorgenfrei-Tornquist Zone.

The sedimentary deposits in the study area were eroded during the late Cenozoic subsequent to their maximum burial during the Neogene. First, erosion occurred during the Miocene–Pliocene in response to uplift of the area and of Scandinavia as a whole as discussed below, and thereafter, glacial erosion was of major importance as witnessed by the large volume of Pleistocene sediments in the North Sea Basin (e.g. Japsen 1998).

The late Cenozoic erosion was followed by Quaternary reburial which in onshore Denmark occurred later than c. 0.3 Ma, the age of oldest Quaternary sediments (Knudsen 1995). The age of the oldest Quaternary deposits is progressively older further into the North Sea, and in the westernmost part of the Danish sector, sedimentation was almost continuos during the late Cenozoic (Konradi 1995; Japsen 1998).

Magnitude of late Cenozoic erosion

The section removed by late Cenozoic erosion, is estimated from data for 68 Danish wells based on a comparison of results from basin modelling (35 wells), and from sonic data (60 wells) (Table 3; Appendix B). Possible local effects due to salt diapirism were not considered.

The estimated missing section reaches and exceeds 1000 m in a number of wells in north-eastern Denmark (Fig. 14). For the Frederikshavn-1 well, both methods estimate a missing section of c. 1000 m, whereas the maximum based on basin modelling alone is 1200 m in the Hans-1 well, and the maximum from sonic data alone is 1300 m in the Sæby-1 well. The latter value is, however, based on data from the F-I Member, and appears to be overestimated when compared to results from neighbouring wells.

The missing section is found to be close to or slightly above 500 m in many Danish wells located in a broad band covering the study area from north-west to south-east. The magnitude of erosion increases clearly along the northern side of the Sorgenfrei-Tornquist Zone (Fig. 1). In the northern part of the zone, estimates of erosion are as high as they are north of the zone, on the Skagerrak-Kattegat Platform, whereas, in the southern part of the zone, estimates of erosion are similar to estimates south of the zone. These differences indicate stronger tectonic movements during the Neogene of the Skagerrak-Kattegat Platform and of the northern part of the Sorgenfrei-Tornquist Zone than in the area to the south.

Missing sections between 250 and 500 m are mapped in the western and southern part of the study area. Erosion estimates of only 100–250 m are found in the south-westernmost part of Jylland. Estimates of 250 m are, however, close to the accuracy of the methods, and the Mesozoic–Cenozoic succession may thus be close to normal compaction in that area. The two easternmost Danish wells with Mesozoic sediments found to be at maximum burial are the L-1 and S-1 wells.

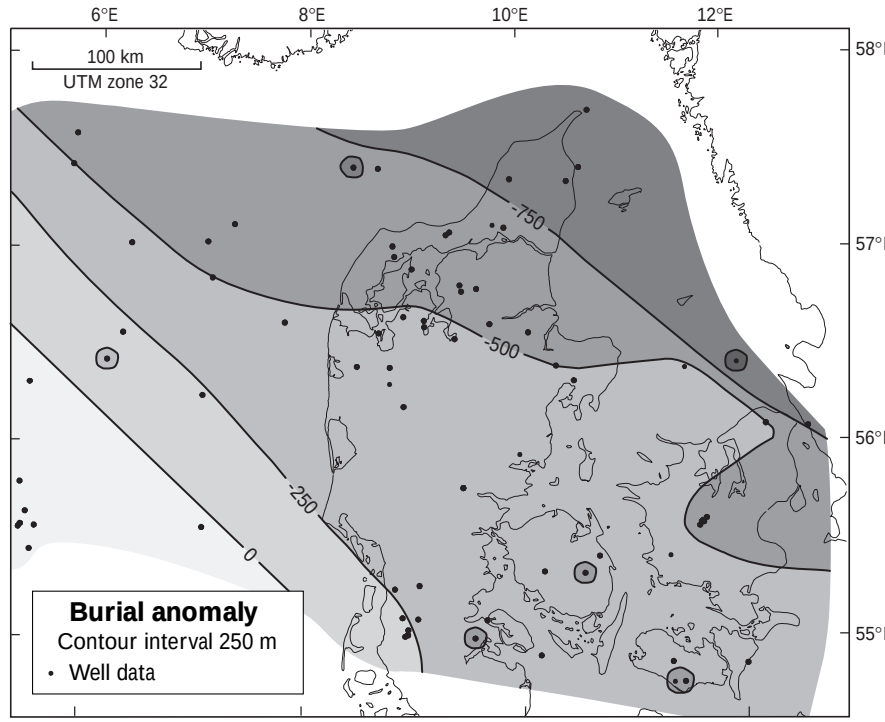

Fig. 15. Map of burial anomaly due to late Cenozoic erosion based on estimates from basin modelling and sonic data (Table 2). The burial anomaly expresses how much the overburden thickness has been reduced since a sedimentary unit was at maximum burial, and this measure of erosion is thus masked by Quaternary re-burial (Equation 2; Fig. 4).

The absence of Upper Pliocene sediments in the L-1 indicates a situation of no-deposition rather than an episode of erosion (Laursen 1992).

The difference between the magnitude of burial anomaly and the missing section is the thickness of the Quaternary (Equation 4; Figs 14, 15). Thick Quaternary deposits are found in northern Jylland and towards the central North Sea, and this is reflected in the smaller magnitudes of the burial anomaly towards north and south-west relative to the missing section.

Comparison with other studies

Three studies from the early 1990's found increasing erosion towards north-east in the area as the present study also concludes, but these studies found the missing section to be substantially greater along the Sorgenfrei-Tornquist Zone (Jensen & Schmidt 1992; 1993; Japsen 1993; Michelsen & Nielsen 1993). The studies by Japsen (1993) and by Michelsen & Nielsen (1993) were based on data from the F-I Member that overestimate erosion towards north-east because of lithological variations, and this may explain part of the discrepancies.

Jensen and Schmidt (1992, 1993) overestimated erosion by an average of c. 450 m relative to the present study for the 14 Danish wells in common; the maximum overestimate is 1000 m. The burial anomalies were estimated from vitrinite reflectance, density and sonic data.

Japsen (1993) overestimated erosion by c. 250 m in average relative to the present study for the 31 wells in common; the maximum overestimate is 1000 m. The estimates of erosion were based on the same data for the F-I Member used here, and calculated relative to a linear velocity-depth trend for Lower Jurassic shale in the Northwest German Basin determined by Scherbaum (1982). This trend deviates less than 100 m from the shale trend applied here for the relevant velocity interval (Equation 4).

Michelsen and Nielsen (1993) overestimated erosion by c. 650 m relative to the present study for the 7 wells in common; the maximum overestimate is 1300 m. The burial anomalies were calculated for the F-I Member relative to a simple exponential transit time-depth trend established by these authors. This trend results in overestimates of erosion by up to 300 m for the relevant velocity interval relative to the trend applied here (Equation 4).

Japsen (1998) overestimated erosion by an average of c. 200 m relative to the present study for the 51 wells in common; the maximum overestimate is 500 m. In the present study, Chalk burial anomalies are calculated relative the revised Chalk baseline (Equation 3), which is shifted towards more shallow depths by c. 200 m for the main velocity interval relative to the Chalk trend applied by Japsen (1998).

Neogene uplift of southern Scandinavia and of the South Swedish Dome

There is a general increase in the amount of erosion observed towards the Norwegian and Swedish coasts (Fig. 14). This matches the increase in the age of the base-Quaternary subcrop in the same direction, and only the base-Quaternary unconformity extents over an area similar to the observed erosion pattern (Fig. 1) (Japsen 1993). These observations provide evidence that the onset of erosion occurred during the Neogene, and indicate that Neogene uplift and erosion has affected not only Norway and Denmark, but also southern Sweden (Japsen 1993).

Lidmar-Bergström (1999) discussed the geomorphological evidence concerning the uplift history of the two surface domes in southern Scandinavia. The Southern Scandes are the most prominent of the domes. They constitute the main part of southern Norway and have a maximum elevation of 2540 m above sea level. There is a general consensus that major uplift of the Southern Scandes occurred in the Neogene, and this is in accordance with a Neogene onset of erosion in northern Denmark (Peulvast 1985; Rohrman et al. 1995; Jensen & Schmidt 1992; Riis 1996; Lidmar-Bergström 1999). Lidmar-Bergström et al. (in press) argued that a Paleogene uplift phase also affected the Southern Scandes.

The South Swedish Dome, which is the smaller of the domes, culminates north-east of the Kattegat, just south of Lake Vättern, and has a maximum elevation of 380 m above sea level (Fig. 1) (Lidmar-Bergström et al. 1993; 1996). On its northern and eastern flanks, the sub-Cambrian peneplain can be traced up to its summit. This extremely flat surface was formed during a period of major denudation, and it is found everywhere on the Baltic Shield (e.g. Högbom & Ahlström 1924; Lidmar-Bergström 1996). To the south and to the west of the South Swedish Dome, the sub-Cambrian peneplain was re-exposed during the warm and humid Mesozoic climate (Lidmar-Bergström 1995). Deep weathering took place and kaolinitic saprolites were formed, and the bedrock surface was changed to a hilly etch-surface. Lidmar-Bergstöm (1996) suggested that this sub-Cretaceous surface is preserved today because it was protected by Cretaceous cover rocks during the Cenozoic. Correspondingly, where the sub-Cambrian peneplain is well-preserved, it must have been protected during the Mesozoic by a Paleozoic cover, and the rise of the South Swedish Dome (and the re-exposure of the sub-Cambrian peneplain) occurred some time during the Cenozoic (Lidmar-Bergström 1995; 1996). In the crestal part of the South Swedish Dome, several occurrences of weathering products suggested to be of Plio–Pleistocene age, have been described (Lidmar-Bergström et al. 1997). These gravelly saprolites differ markedly from the kaolinitic saprolites associated with the pre-Cenozoic weathering. In the south-western part of the South Swedish Dome, the flat South Småland Surface has cut off the inclined sub-Cretaceous surface, and it is thought that it developed during the Cenozoic after erosion of the Cretaceous cover (Lidmar-Bergström 1995; 1996).

Additional information is obtained when these observations from the exposed basement in southern Sweden are combined with geologic evidence from the sedimentary cover in the adjacent areas in eastern Denmark, e.g. Sjælland, where Paleocene sediments are preserved, and a Cenozoic cover of c. 500 m has been removed (Figs 1, 14). Neogene uplift of the entire southern Scandinavia, centred around the South Swedish Dome, could explain these occurrences, and be in agreement with the geomorphological evidence. Furthermore, Neogene uplift must have affected the vast areas to the north and east of the Dome where the sub-Cambrian peneplain is exposed today, and the sub-Cretaceous surface south and west of the Dome could be preserved due to Paleogene cover rocks removed by Neogene erosion. The removal of c. 1 km of mainly Paleogene sediments from southern Sweden during the Neogene is a possible interpretation of fission track data acquired in that area (compare Cederbom 1997). In Denmark, the uplift of the basement led to the erosion of Cenozoic cover rocks in large parts of the territory.

A rise of the South Swedish Dome during the Neogene is consistent with the clockwise shift in sediment transport directions that are observed in the north-eastern North Sea Basin ranging from the north (Oligocene–Early Miocene) to the north-east (Late Miocene) and finally to the east (Pliocene) (Fig. 1) (Clausen et al. 1999). The occurrence of gibbsite in the Gram Formation indicates erosion of tropical soil during the Late Miocene, and a short fluvial transport as the mineral is unstable in fresh water (Rasmussen & Larsen 1989). The Late Miocene sediments found in south-western Denmark may thus be sourced from Sweden or the Skagerrak-Kattegat Platform. It should also be noted that Larsen & Dinesen (1959) found that the content of heavy minerals in the sediments supplied to the Danish area changed during the Miocene.

The suggested Plio–Pleistocene age of the weathering products found on the crestal part of the South Swedish Dome are consistent with Neogene uplift of the Dome, whereas the Oligocene transport direction from the north in the North Sea Basin corresponds to a Paleogene uplift phase of the Southern Scandes (Lidmar-Bergström et al. 1997, in press; Clausen et al. in press).

Discussion and conclusions

The combination of basin modelling and analysis of sonic data to estimate erosion minimises the uncertainty of the estimates by identifying outlying values,

and extends the areal coverage relative to the application of a single method. We thus estimate erosion to be in average 200–600 m lower than previous studies. We also find erosion estimates based on Chalk velocities to be in good agreement with estimates based on basin modelling, and this must be due to the homogenous composition of the Chalk, and the relative thick section used for the calculation of the mean velocity of the Chalk in most wells. Basin modelling predicts heat flow variation for the Oligocene–Recent time interval in order to match the steep vitrinite reflectance gradient and the present-day temperature. This is suggested to be due to transient effects induced by rapid deposition and erosion.

The missing section removed by late Cenozoic erosion increases towards north-east in Denmark. We estimate the erosion to be c. 500 m in a broad zone across the country from north-west to south-east which in particular covers the locality at Stevns Klint. This zone largely conforms with the areas where Paleocene deposits subcrop the Quaternary, and the eroded sediments must thus have been of mainly Paleocene-Miocene age.

Further south-west of this intermediate zone, erosion declines towards zero in the western and southern part of the Danish North Sea. The age of the removed sediments must have been progressively younger in this direction. The missing section reaches 1000–1200 m on and along the Skagerrak-Kattegat Platform. Where the Chalk is preserved on the Platform, the missing section is thus likely to be c. 500 m of Cenozoic sediments as south of the area plus a Chalk section of c. 500 m.

The deep erosion on and along the Skagerrak-Kattegat Platform cannot be explained by glacial erosion, and this documents that Denmark was affected by tectonic uplift during the Neogene. The pattern of late Cenozoic erosion in Denmark agrees with a Neogene uplift of south Norway centred around the southern Scandes and of south-east Scandinavia centred around the South Swedish Dome.

Acknowledgements

The study was made possible through the generous support of the Carlsberg Foundation and GEUS. We are thankful for inspiring discussions with Charlotte Cederbom (University of Göteborg), Ole Graversen (University of Copenhagen), Karna Lidmar-Bergström (University of Stockholm), James A. Chalmers, Ulrik Gregersen, Peter Konradi, Anders Mathiesen, Lars Henrik Nielsen, Erik Skovbjerg Rasmussen and Ole Vejbæk (all GEUS) and for the comments by reviewers Lars Nørgaard Jensen (Statoil, Norway) and Søren Bom Nielsen (University of Århus).

Dansk sammendrag

Vi anslår mægtigheden af de dæklag der er blevet borteroderet sent i Kænozoikum ud fra bassinmodellering og lydmålinger i 68 danske boringer, og vi når frem til mindre værdier end i tidligere undersøgelser. Mægtigheden af de borteroderede dæklag vokser fra nul i den vestlige og sydlige del af dansk Nordsø til 1000–1200 m i det nordøstlige Danmark. I en bred zone mangler ca. 500 m palæocæne til miocæne aflejringer, der hvor palæocæne sedimenter ligger under de kvartære aflejringer. På Skagerrak-Kattegat Platformen er yderligere ca. 500 m Skrivekridt blevet borteroderet, hvor de nedre dele af kridtet stadig er bevaret, mens de borteroderede sedimenter må have været yngre mod sydvest, hvor miocæne aflejringer ligger under de kvartære aflejringer. Den dybe erosion på og langs med Skagerrak-Kattegat Platformen viser at neogen landhævning og erosion påvirkede området inden den glaciale erosion i kvartær tid. Disse resultater stemmer overens med neogen landhævning af det sydlige Norge samt af det sydlige Sverige centreret om Den Sydsvenske Dome hvis højdepunkt befinder sig nordøst for Kattegat.

References

Bertelsen, F. 1980: Lithostratigraphy and depositional history of the Danish Triassic. Geological Survey of Denmark B 4, 59 pp.

Buchardt, B. 1978: Oxygen isotope paleotemperatures from the Tertiary period in the North Sea area. Nature 275, 121–123.

Bulat J. & Stoker S. J. 1987: Uplift determination from interval velocity studies, UK, southern North Sea. In Brooks, J. & Glennie, K. W. (eds), 293–305. London: Graham & Trotman.

Cederbom, C. 1997: Fission track thermochronology applied to Phanerozoic thermotectonic events in central and southern Sweden. 47 pp. Göteborg University, Licentiate degree.

Clausen, O. R., Gregersen, U., Michelsen, O. & Sørensen, J. C. 1999: Factors controlling the Cenozoic sequence development in the eastern parts of the North Sea. Journal of the Geological Society London 156, 809–816.

Clausen, O. R., Nielsen, O. B., Huuse, M. & Michelsen, O. in press: Geological indications for Palaeogene uplift in the eastern North Sea Basin. Global & Planetary Change.

Fredén, C. 1994: Geology. National Atlas of Sweden. 208 pp. Stockholm: SNA Publishing.

Haq, B. U., Hardenbol, J. & Vail, P. R. 1987: Chronology of fluctuating sea levels since the Triassic. Science 235, 1156–1167.

Harland, W. B., Armstrong, R. L., Cox, A.V., Craig, L. E., Smith, A. G. & Smith, D. G. 1990: A geologic time scale 1989. Cambridge: Cambridge University Press.

Hillis, R. R. 1995: Quantification of Tertiary exhumation in the United Kingdom southern North Sea using sonic velocity data. AAPG Bulletin 79, 130–152.

Högbom, A. G. & Ahlström, N. G. 1924: Über die sub-

kambrische Landfläche am fusse vom Kinnekulle. Bulletin of the Geological Institution of the University of Uppsala 19, 55–88.
Iliffe, J. E. & Dawson, M. R. 1996: Basin modelling history and predictions. In Glennie, K.W. & Hurst, A. (eds) 1995: NW Europe's Hydrocarbon Industry. 83–105. London: Geological Society.
Japsen, P. 1993: Influence of lithology and Neogene uplift on seismic velocities in Denmark; implications for depth conversion of maps. AAPG Bulletin 77, 194–211.
Japsen, P. 1998: Regional velocity-depth anomalies, North Sea Chalk: a record of overpressure and Neogene uplift and erosion. AAPG Bulletin 82, 2031–2074.
Japsen, P. in press: Investigation of multi-phase erosion using reconstructed shale trends based on sonic data. Sole Pit axis, North Sea. Global and Planetary Change.
Jensen, L. N. & Schmidt, B. J. 1992: Late Tertiary uplift and erosion in the Skagerrak area; magnitude and consequences. Norsk Geologisk Tidsskrift 72, 275–279.
Jensen L. N. & Schmidt B. J. 1993: Neogene uplift and erosion offshore South Norway; magnitude and consequences for hydrocarbon exploration in the Farsund Basin. In Spencer, A. M. (ed.) Generation, accumulation, and production of Europe's hydrocarbons; III, 79–88. Berlin Heidelberg: Springer Verlag.
Knudsen, K. L. 1995: Kvartæret. In Nielsen, O. B. (ed.) Danmarks geologi fra Kridt til i dag. 247–269. Århus: Aarhus Universitet.
Konradi P. 1995: Foraminiferal biostratigraphy of the post mid-Miocene in two boreholes in the Danish North Sea. In Michelsen, O. (ed.) Proceedings of the 2nd symposium on Marine Geology. Geological Survey of Denmark C 12, 101–112.
Larsen, G. 1966: Geologiske resultater af bundundersøgelserne i Øresund. Meddelser fra Dansk Geologisk Forening 16, 260–265.
Larsen, G. & Dinesen, A. 1959: Vejle Fjord Formationen ved Brejning. Danmarks Geologiske Undersøgelse II. række 82.
Laursen, G. V. 1992: Foraminifera of the eastern North Sea. In Laursen, G. V., Heilmann-Clausen, C. & Thomsen, E. (eds) Cenozoic biostratigraphy of the eastern North Sea based on foraminifera, dinoflagellates, and calcareous nannofossils. 1–68. Århus: Geologisk Institut.
Liboriussen, J., Ashton, P. & Tygesen, T. 1987: The tectonic evolution of the Fennoscandian Border Zone in Denmark. Tectonophysics 137, 21–29.
Lidmar-Bergström, K. 1995: Relief and saprolites through time on the Baltic Shield. Geomorphology 12, 45–61.
Lidmar-Bergström, K. 1996: Long term morphotectonic evolution in Sweden. Geomorphology 16, 33–59.
Lidmar-Bergström, K. in press: Uplift histories revealed by landforms of the Scandinavian domes. Uplift, Erosion and Stability.
Lidmar-Bergström, K., Kleman, J. & Rapp, A. 1993: Geomorphology in Sweden. In Walker, H.-J. & Grabau-Warren, E. (eds) The evolution of geomorphology; a nation-by nation summary of development. 415–428. Chichester: John Wiley and Sons.
Lidmar-Bergström, K., Ollier, C. D. & Sulebak, J. C. in press: Landforms and uplift history of southern Norway. Global and Planetary Change.
Lidmar-Bergström, K., Olsson, S. & Olvmo, M. 1997: Palaeosurfaces and associated saprolites in southern Sweden. In Widdowson, M. (ed.) Palaeosurfaces; recognition, reconstruction and palaeoenvironmental interpretation. Geological Society Special Publication 120, 95–124.
Lindgreen, H. 1991: Elemental and structural changes in illite/smectite mixed-layer clay minerals during diagenesis in Kimmeridgian- Volgian (- Ryazanian) clays in the Central Trough, North Sea and the Norwegian-Danish Basin. Bulletin of the Geological Society of Denmark 39, 1–82.
Michelsen, O. 1989: Revision of the Jurassic lithostratigraphy of the Danish subbasin. Geological Survey of Denmark A 24, 21 pp.
Michelsen, O. & Nielsen, L. H. 1993: Structural development of the Fennoscandian border zone, offshore Denmark. Marine and Petroleum Geology 10, 124–134.
Nielsen, L. H. & Japsen, P. 1991: Deep wells in Denmark, 1935-1990; lithostratigraphic subdivision. Geological Survey of Denmark A 31. 179 pp.
Nielsen, O. B., Sørensen, S., Thiede, J. & Skarbo, O. 1986: Cenozoic differential subsidence of North Sea. AAPG Bulletin 70, 276–298.
Pedersen, G. K. 1985: Thin, fine-grained storm layers in a muddy shelf sequence: an example from the Lower Jurassic in the Stenlille 1 well, Denmark. Journal of the Geological Society London 142, 357–374.
Peulvast, J.-P. 1985: Post-orogenic morphotectonic evolution of the Scandinavian Caledonides during the Mesozoic and Cenozoic. In Gee, D. G. & Sturt, B. A. (eds) The Caledonide Orogen – Scandinavia and related areas. 979–996. Chichester: Wiley and Sons.
Rasmussen, E. S. & Larsen, O. 1989: Mineralogi og geokemi af det Øvre Miocæne Gram ler. Danmarks Geologiske Undersøgelse D 7. 80 pp.
Rasmussen, L. B. 1961: De miocæne formationer i Danmark. Danmarks Geologiske Undersøgelse IV. række 4. 45 pp.
Riis, F. 1996: Quantification of Cenozoic vertical movements of Scandinavia by correlation of morphological surfaces with offshore data. Global & Planetary Change 12, 331–357.
Riis, F. & Jensen, L. N. 1992: Introduction; Measuring uplift and erosion; proposal for a terminology. Norsk Geologisk Tidsskrift 72, 223–228.
Rohrman, M., van der Beek, P., Andriessen, P. & Cloetingh, S. 1995: Meso-Cenozoic morphotectonic evolution of southern Norway: Neogene domal uplift inferred from apatite fission track thermochronology. Tectonics 14, 700–714.
Scherbaum, F. 1982: Seismic velocities in sedimentary rocks; indicators of subsidence and uplift. Geologische Rundschau 71, 519–536.
Sorgenfrei, Th. & Buch, A. 1964: Deep test in Denmark, 1935–1959. Geological Survey of Denmark, III række 36, 146 pp.
Spjeldnæs, N. 1975: Palaeogeography and facies distribution in the Tertiary of Denmark and surrounding areas. Norges Geologiske Undersøgelse Bulletin 316, 289–311.
Urmos, J., Wilkens, R. H., Bassinot, F., Lyle, M., Marsters, J. C., Mayer, L. A. & Mosher, D. C. 1993: Laboratory and well-log velocity and density measurements from the Ontong Java Plateau. In Berger, W. H., Kroenke, L. W., Mayer, L. A. & Janecek, T. R. (eds) Proceedings of the Ocean Drilling Program. Scientific results. 130, 607–622. College Station: Ocean Drilling Program.
Vejbæk, O. V. & Britze, P. 1994: Geological map of Den-

mark. 1:750 000. Top pre-Zechstein (two-way traveltime and depth). Geological Survey of Denmark. Map Series 45, 5 maps and 8 pp.
Vik, E. & Hermanrud, C. 1993: Transient thermal effects of rapid subsidence in the Haltenbanken area. In Doré, A.G., Augustson, J.H., Hermanrud, C., Stewart, D. J. & Sylta, O. (eds) Basin Modelling: Advances and Applications. Norwegian Petroleum Society (NPF), Special Publication 3, 107–117. Amsterdam: Elsevier.
Yükler, M. A. 1978: One-dimensional model to simulate geologic, hydrodynamic and thermodynamic development of a sedimentary basin. Geologische Rundschau 67, 960–979.

Appendix A – Normal velocity-depth trends for different formations

A revised normal velocity-depth trend for the North Sea Chalk

Japsen (1998) published a normal velocity-depth trend for the Chalk Group based on an analysis of 845 wells throughout the North Sea Basin and ODP data. For the shallowest part of the trend, no data representing normal compaction were found for the Chalk of the North Sea Basin, so sonic log data from Eocene to Recent ooze and chalk deposits from a stable platform were used to guide the trend (Urmos et al. 1993). At intermediate depths, Japsen (1998) applied qualitative arguments to identify North Sea data representing normal compaction along the lower bound for velocity-depth data for which the effect of overcompaction due to erosion is minimum. At greater depths, data representing normal compaction were identified along the upper bound where the effect of undercompaction due to overpressuring is a minimum.

However, Japsen (in press) found additional geological constraints to refine the identification of reference data at intermediate depths where the influence of erosion and overpressuring is difficult to ascertain. Because the sonic method identifies deviations from maximum burial, post-erosional reburial of a formation will reduce its observable burial anomaly; e.g. a pre-Quaternary erosion of 500 m will be masked by a subsequent Quaternary reburial of 500 m (Equation 2). This implies that where the Quaternary is thick, even minor deviations from maximum burial due to late Cenozoic erosion may correspond to a substantial missing section. Deep erosion is, however, not likely where the base-Quaternary hiatus is minor, e.g. where the Quaternary is underlain by Neogene sediments.

Normally–compacted Chalk is thus likely to be found in areas where the Quaternary is thick, Neogene deposits are present and pressure is hydrostatic. Consequently, the normal velocity-depth trend for the North Sea Chalk should follow the upper bound for data from such areas, whereas data representing undercompaction due to overpressuring should plot below the trend. A revised baseline was thus defined by Japsen (in press) by such maximum velocity data for $900<z<1700$ m. The revised trend lines up with the maximum velocity data used to define the original trend for $z>$in press m, and with a velocity at the surface of 1550 m/s:

$$\begin{aligned} V_N^{Ch} &= 1550 + 1.3 \cdot z, && z < 900 \text{ m} \\ V_N^{Ch} &= 920 + 2 \cdot z, && 900 < z < 1471 \text{ m} \\ V_N^{Ch} &= 1950 + 1.3 \cdot z, && 1471 < z < 2250 \text{ m} \\ V_N^{Ch} &= 2625 + z, && 2250 < z < 2875 \text{ m} \end{aligned} \quad (3)$$

The fourth of the above segments is unchanged from the original trend, in which the upper three segments were formulated as $1600+z$, $500+2z$, and $937.5+1.75z$ (Japsen 1998). The revised trend is shifted towards shallower depths by a mean of 160 m for the velocity interval affected by the revision and where North Sea data are found, $2100<V<4875$ m/s; the maximum shift is 210 m for $2920<V<3920$ m/s.

The shift towards higher velocities for the revised baseline results in a reduction in estimates of erosion by up to 210 m, and an increase in estimates of overpressure by up to 2 MPa for data points that plot above and below the line respectively (overcompaction due to overpressure: $dZ_B/100=210/100$ MPa $\approx$2 MPa; see Japsen 1998). The increased overpressure that the revised model predicts, is an improvement relative to the original model which explained only 80% of the observed overpressure in the Chalk for 52 wells located away from diapirs and where the overpressure exceeded 4 MPa (Japsen 1998). The corresponding percentage based on the revised baseline is 91%. This improvement is particularly clear for data from relatively shallow depth/moderate overpressure; e.g. the Danish Dan field where overpressure is 7.3 MPa, and for which the overpressure prediction from velocity data has been increased from 4.3 to 6.5 MPa.

A baseline for marine shale of the Lower Jurassic F-I Member

Japsen (in press) formulated a constrained baseline, V_N^{LJur}, for marine shale dominated by smectite/illite based on velocity-depth data for the Lower Jurassic F-1 Member from 31 Danish wells of which 28 have data for the Chalk (Fig. 6):

$$tt = 460 \cdot e^{-z/2175} + 185 \quad (4)$$

The baseline was reconstructed by correcting present formation depths for the effect of late Cenozoic erosion as estimated from the velocity of the overlying chalk in these wells relative to the revised Chalk trend (Equation 3). The corrected depths correspond to the burial of the formation prior to Neogene erosion when the sediments were at maximum burial at more lo-

cations. The baseline can thus be traced more easily in a plot of velocity versus the corrected depths, and is well defined at great depth, where velocity-depth data for normally compacted shale at maximum burial can be difficult to identify (2.1<z<3.8 km). This formulation is a constrained, exponential transit time-depth model that fulfils reasonable boundary conditions at the surface and at infinite depth; V_0=1550 m/s and V_∞=5405 m/s; the maximum velocity-depth gradient is 0.6 m/s/m for *z*=2.0 km.

A baseline for the Lower Triassic Bunter Shale

Japsen (in press) formulated a segmented, linear baseline, V_N^{BSh}, for the Lower Triassic Bunter Shale based on velocity-depth data from 142 British and Danish wells of which 91 have velocity-depth data for the Chalk (Fig. 7):

$$\begin{aligned} V_N^{BSh} &= 1550 + z \cdot 0{,}6, && 0 < z < 1393 \text{ m} \\ V_N^{BSh} &= -400 + z \cdot 2, && 1393 < z < 2000 \text{ m} \\ V_N^{BSh} &= 2600 + z \cdot 0{,}5, && 2000 < z < 3500 \text{ m} \\ V_N^{BSh} &= 3475 + z \cdot 0{,}25, && 3500 < z < 5300 \text{ m} \end{aligned} \quad (5)$$

The trend indicates a pronounced variation of the velocity gradient with depth: The gradient is only 0.5 m/s/m in the upper part, and increases to 1.5 m/s/m for depths around 2 km, from where it decreases gradually with depth to 0.5 and then 0.25 m/s/m.

The Bunter Shale baseline was reconstructed by applying the same procedure as for the lower Jurassic shale by correcting present formation depths for the effect of late Cenozoic erosion as estimated from Chalk velocities. The trend was constructed to predict likely values near the surface (V_0=1550 m/s), and is based on reference data with corrected depths from 1600 to 5600 m (Japsen in press).

Rather than proposing a specific baseline for the Lower Triassic Bunter Sandstone, Japsen (in press) suggested that the trend formulated for the Bunter Shale was a reasonable approximation for a data set from 133 British and Danish wells of which 87 have velocity-depth data for the Chalk (see Fig. 7). Data from shale is preferable to those from sandstone for studies of maximum burial for several reasons: Shale porosity is less affected by diagenetic processes, shale does not act as an aquifer with the consequent porosity variations, and shale may be more uniform in regard to both grain size and to mineralogy. Burial anomalies for the Bunter Sandstone can thus be used to place an upper limit on estimates of erosion based on Bunter Shale data.

The dominance of smectite/illite in the distal parts of the Fjerritslev Formation (H. Lindgreen, personal communication 1998), and of kaolin in the continental Bunter Shale was suggested by Japsen (in press) to be a possible explanation why these two baselines diverge, and why those for the Bunter Shale and Bunter Sandstone converge at depth.

Appendix B – Calculation of estimates of erosion

Burial anomaly estimated from sonic data

A single burial anomaly due to late Cenozoic erosion, ${}^{Neo}dZ_B^{sonic}$, is estimated for 60 wells based on burial anomalies, dZ_B^{Ch}, dZ_B^{LJur}, dZ_B^{BSs} and dZ_B^{BSh}, calculated from sonic data for the Chalk, the lower Jurassic F-I Member, the Bunter Sandstone and the Bunter Shale (Fig. 16; Table 2).

Step 1. A single, Triassic burial anomaly, dZ_B^{Tr}, is computed for each well where data for the Bunter Sandstone or the Bunter Shale are available (22 wells). The value is generally set equal to the Bunter Shale value (12 wells) because shale is considered to be more uniform than sandstone. However, to be conservative it is set to the Bunter Sandstone value when the Shale value exceeds the Sandstone value by more than 400 m (3 wells) or if no Bunter Shale value is available (6 wells). For the Felicia-1 well, the Bunter Shale value was found to be the most likely, and for the Rødby-2 well, the Triassic data were found to result in a too high estimate of erosion.

Step 2. A single, pre-Chalk burial anomaly, dZ_B^{pre-Ch}, is computed for each well where data for the Triassic or for the lower Jurassic are available (50 wells). Data for both levels occur only in 3 wells for which the mean of the estimates is computed; in the remaining wells the pre-Chalk anomaly is set equal to either the Triassic or the lower Jurassic anomaly.

Step 3. A single burial anomaly due to late Cenozoic erosion based on sonic data, ${}^{Neo}dZ_B^{sonic}$, is either set equal to dZ_B^{Ch} (10 wells), dZ_B^{pre-Ch} (8 wells) or computed based on a comparison of dZ_B^{pre-Ch} and dZ_B^{Ch} (42 wells) (Fig. 13):

- If $-250 < dZ_B^{pre-Ch} - dZ_B^{Ch} < 250$ m, we take ${}^{Neo}dZ_B^{pre-Ch}$ as the mean of dZ_B^{pre-Ch} and dZ_B^{Ch} (32 wells); the weight of the estimate from Chalk data is set to twice that based on pre-Chalk data.
- If $dZ_B^{pre-Ch} - dZ_B^{Ch} > 250$ m, we take ${}^{Neo}dZ_B^{sonic} = dZ_B^{Ch}$; impossible in the ideal case, so the Chalk estimate is considered more reliable (2 wells).
- If $dZ_B^{pre-Ch} - dZ_B^{Ch} < -250$ m, we take ${}^{Neo}dZ_B^{sonic} = dZ_B^{Ch}$; the Chalk estimate represents the conservative choice, and the magnitude of the pre-Chalk estimate may in theory reflect a pre-Chalk erosional event (8 wells).

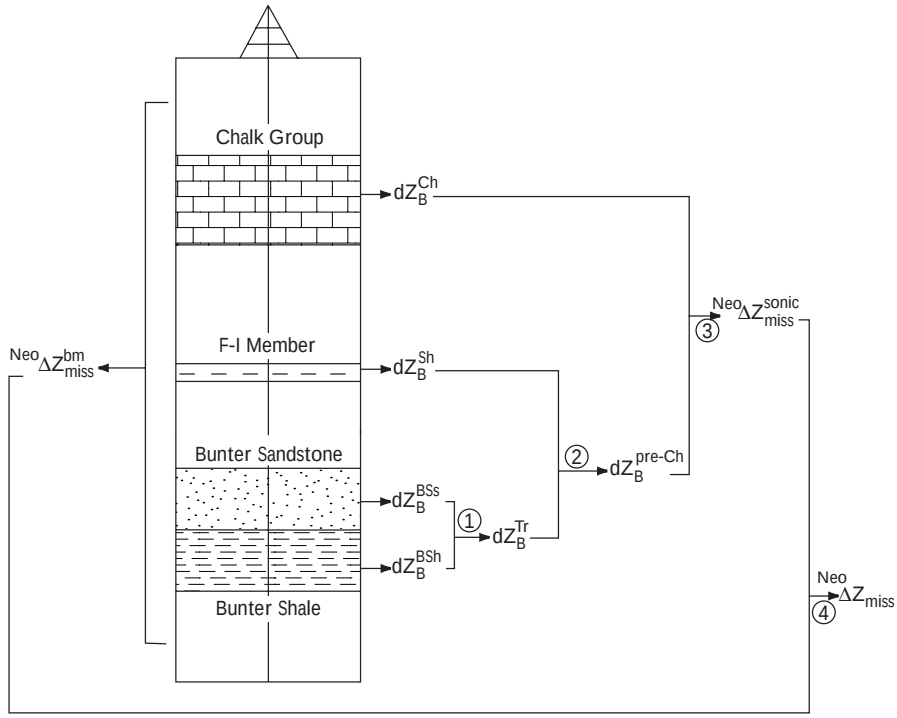

Fig. 16. Decision tree illustrating the calculation of the missing section due to late Cenozoic erosion, $^{Neo}\Delta Z_{miss}$, based on estimates from basin modelling and sonic data, $^{Neo}\Delta Z_{miss}^{bm}$ and $^{Neo}\Delta Z_{B}^{sonic}$. The missing section is found by correcting the burial anomaly for the Quaternary reburial (Fig. 4, Equation 2). Symbols are explained in Table 1. See Appendix B for details.

Missing section as estimated from basin modelling and sonic data

The output from the analysis of the sonic data, the burial anomaly due to late Cenozoic erosion, $^{Neo}dZ_B^{sonic}$, is corrected for the Quaternary reburial to obtain an estimate of the missing section, ΔZ_{miss}^{sonic} (Equation 2). This value is then compared to the output from the basin modelling programme, an estimate of the missing section removed by late Cenozoic erosion, $^{Neo}\Delta Z_{miss}^{bm}$.

Step 4. A single estimate of the missing section removed by late Cenozoic erosion, $^{Neo}\Delta Z_{miss}$, is computed for 68 wells. The estimate is either set equal to $^{Neo}\Delta Z_{miss}^{sonic}$ (33 wells), $^{Neo}\Delta Z_{miss}^{bm}$ (8 wells) or obtained from a comparison of estimates based on sonic data and on basin modelling (27 wells):

- If $-250 < {}^{Neo}\Delta Z_{miss}^{sonic} - {}^{Neo}\Delta Z_{miss}^{bm} < 250$ m, we take $^{Neo}\Delta Z_{miss}$ as the mean value of the two estimates (23 wells).
- If $^{Neo}\Delta Z_{miss}^{sonic} - {}^{Neo}\Delta Z_{miss}^{bm} > 250$ m, we take a conservative choice $^{Neo}\Delta Z_{miss} = {}^{Neo}\Delta Z_{miss}^{bm}$ (3 wells).
- $^{Neo}\Delta Z_{miss}^{sonic} - {}^{Neo}\Delta Z_{miss}^{bm}$ is less than –250 m for the Børglum-1 well, and in this case we take $^{Neo}\Delta Z_{miss} = {}^{Neo}\Delta Z_{miss}^{bm}$. The basal part of the Upper Cretaceous is highly dominated by clay and claystone in this well, and $^{Neo}\Delta Z_{miss}^{sonic}$ is thus probably underestimated because it is based on Chalk data (Sorgenfrei & Buch 1964).